PRODUCTION OF AEROGEL-MODIFIED EXPANDED PERLITE AGGREGATE AND CLAY (AEP/C) BOARD AND INVESTIGATION OF PHYSICAL AND MECHANICAL PROPERTIES

A Master's Thesis

by
ELİF MERCAN

Department of
Interior Architecture and Environmental Design
İhsan Doğramacı Bilkent University
Ankara
July 2021

PRODUCTION OF AEROGEL-MODIFIED EXPANDED PERLITE AGGREGATE AND CLAY (AEP/C) BOARD AND INVESTIGATION OF PHYSICAL AND MECHANICAL PROPERTIES

The Graduate School of Economics and Social Sciences
of
İhsan Doğramacı Bilkent University

by

ELİF MERCAN

In Partial Fulfillment of the Requirements for the Degree of
MASTER OF FINE ARTS

in

DEPARTMENT OF
INTERIOR ARCHITECTURE AND ENVIRONMENTAL DESIGN
İHSAN DOĞRAMACI BİLKENT UNIVERSITY
ANKARA

July 2021

I certify that I have read this thesis and have found that it is fully adequate, in scope and in quality, as a thesis for the degree of Master of Arts in Interior Architecture and Environmental Design.

_____
Assoc. Prof. Dr. Semiha Yılmazer
Supervisor

I certify that I have read this thesis and have found that it is fully adequate, in scope and in quality, as a thesis for the degree of Master of Arts in Interior Architecture and Environmental Design.

_____
Asst. Prof. of Practice Burçak Altay
Examining Committee Member

I certify that I have read this thesis and have found that it is fully adequate, in scope and in quality, as a thesis for the degree of Master of Arts in Interior Architecture and Environmental Design.

_____
Prof. Dr. Cüneyt Kurtay
Examining Committee Member

I certify that I have read this thesis and have found that it is fully adequate, in scope and in quality, as a thesis for the degree of Master of Arts in Interior Architecture and Environmental Design.

_____
Asst. Prof. of Practice Zühre Sü Gül
Examining Committee Member

Approval of the Graduate School of Economics and Social Sciences

_____
Prof. Dr. Refet Soykan Gürkaynak
Director

ABSTRACT

PRODUCTION OF AEROGEL-MODIFIED EXPANDED PERLITE AGGREGATE AND CLAY (AEP/C) BOARD AND INVESTIGATION OF PHYSICAL AND MECHANICAL PROPERTIES

Mercan, Elif

M.F.A., Department of Interior Architecture and Environmental Design

Supervisor: Assoc. Prof. Dr. Semiha Yılmazer

July 2021

Expanded perlite aggregate (EPA) is an inorganic insulation material preferred because of its low thermal conductivity. In other respects, it has disadvantages in buildings because of its high moisture retention, sintering in case of fire, and fragility. This study aims to produce a clay-based insulation board by eliminating these disadvantages of EPA with aerogel modification. The sol-gel method was chosen, allowing low-cost aerogel synthesis in a laboratory and permitting the control of parameters throughout the process. The optimum synthesis process

was designed by examining the acid and base variables in the process. The recipe obtained at the aerogel synthesis was used to constitute aerogel-modified expanded perlite aggregate (AEP). AEP particles were prepared with clay matrix under determined process conditions, and characterization tests were carried out. According to the results, aerogel modification prevents high-temperature sintering of EPAs. The AEPs and the aerogel-modified expanded perlite aggregate and clay (AEP/C) composites' density remained almost unchanged compared to the EPA and expanded perlite aggregate and clay (EP/C) control samples. Thus, this can be offered that the prepared boards are lightweight and can maintain low thermal conductivity. The results showed that the mechanical strength of the boards was slightly higher than the control samples and the aerogel modification has almost no effect on mechanical strength.

Keywords: Aerogel, Expanded Perlite Aggregate, Sol-Gel Method, Thermal Insulation Board

ÖZET

AEROGEL MODİFİYE EDİLMİŞ GENİŞLETİLMİŞ PERLİT AGREGA VE KİL (GPA/K) LEVHA ÜRETİMİ İLE FİZİKSEL VE MEKANİK ÖZELLİKLERİNİN İNCELENMESİ

Mercan, Elif

Yüksek Lisans, İç Mimarlık ve Çevre Tasarımı Bölümü

Tez Danışmanı: Doç. Dr. Semiha Yılmazer

Temmuz 2021

Genleştirilmiş perlit agregası (GPA) düşük termal iletkenliği sebebiyle tercih edilen bir inorganik yalıtım malzemesidir. Öte yandan, yüksek nem tutuculuğu, yangın durumlarında büzülmesi ve yüksek kırılgan yapısı sebebiyle yapılarda dezavantaj oluşturmaktadır. Bu çalışmada, GPA'nın bu dezavantajlarını aerojel modifikasyonu ile gidererek kil matrisi ile birlikte yalıtım plakası üretmek hedeflenmiştir. Laboratuvar ortamında düşük bütçeli aerojel sentezine imkan

veren ve proses boyunca parametrelerin kontrolüne izin veren sol-jel metodu seçilmiştir. Sol-jel prosesindeki asit ve baz değişkenleriyle optimum sentez süreci tasarlanmıştır. Sentez sonunda elde edilen reçete aerojelle modifiye edilmiş GPA içinde ve üretmek için kullanılmıştır. Aerojel ile modifiye edilmiş GPA partikülleri kil matrisi ile uygun koşullarda hazırlanarak karakterizasyon testleri yapılmıştır. Elde edilen sonuçlara göre, aerojel modifikasyonu GPA'ların yüksek ısıda sinterlenmesinin önüne geçmektedir. Aerojelle modifiye edilmiş genleştirilmiş perlit agregalarının (AGP) ve bu AGP'lerle hazırlanan aerojelle modifiye edilmiş genleştirilmiş perlit/kil (AGP/K) kompozit plakasının yoğunluğu, genleştirilmiş perlit agregası (GPA) ve kil ile hazırlanan genleştirilmiş perlit/kil (GP/K) kontrol numunelerine kıyasla çok az değişmiştir. Böylece, hazırlanan plakaların hafif olduğu ve düşük termal iletkenliğin koruyabileceği söylenebilir. Sonuçlar, levhaların mekanik mukavemetinin kontrol numunelerinden çok az yüksek olduğunu ve aerojel modifikasyonunun mekanik mukavemet üzerinde neredeyse hiçbir etkisi olmadığını göstermiştir.

Anahtar Kelimeler: Aerojel, Genleştirilmiş Perlit Aggregası, Sol-Jel Metodu, Isı Yalıtım Plakası

ACKNOWLEDGMENTS

First and foremost, I would like to express my sincere gratitude to Assoc. Prof. Semiha Yılmazer her encouragement, patience, supervision throughout this study, and endless help to make real my dreams. I would also like to thank all examining committee members for their patience and valuable feedback. I want to thank Cengiz Yılmazer for his courage and patience throughout this research and his important sharing.

I owe my gratitude to my friends Gözde Odabaş, Bartu Lokumcu, Hafize Ürüşan, and Necati Telli for their endless support. Sincere and special thanks to Volkan Acun for his support and assistance in every obstacle I encountered during the research.

Finally, I would like to thank my parents, Gülser and Zeki Mercan, for their compassionate approach and endless support throughout my life. In addition, I want to thank all the authors who have contributed to me in the field of alchemy.

TABLE OF CONTENTS

LIST OF TABLES

LIST OF FIGURES

LIST OF ABBREVIATIONS

AEP	Aerogel-Modified Expanded Perlite
AEP/C	Aerogel-Modified Expanded Perlite/Clay
AGP	Aerojelle Modifiye Edilmiş Genleştirilmiş Perlit
AGP/K	Aerojelle Modifiye Edilmiş Genleştirilmiş Perlit/Kil
ASR	Alkali-Silica Reaction
DH_2O	Distilled Water
EtOH	Ethanol
EPA	Expanded Perlite Aggregate
EP/C	Expanded Perlite Aggregate/Clay
EPS	Expanded Polystyrene
GPA	Genleştirilmiş Perlit Agregası
GP/K	Genleştirilmiş Perlit/Kil
HVAC	Heating, Ventilation and Air Conditioning
SG	Specific Gravity
Si	Silica

TEOS	Tetraethyl Orthosilicate
TMCS	Trimethylchlorosilane
UVM	Unit Volume Mass

CHAPTER I

INTRODUCTION

An upsurge in global energy consumption results from a striking increase in urban and industrial activities depending on the rapid growth of population size (Kalhor & Emaminejad, 2020). The energy need in developing countries has increased since new building constructions (Bribián, Capilla, & Usón, 2011). The energy efficiency in buildings and construction sustainability is apparent due to the increasing environmental pollution and climate change concerns (Cox, Betts, Jones, Spall, & Totterdell, 2000; Ioppolo, Cucurachi, Salomone, Saija, & Shi, 2016; Ortiz, Castells, & Sonnemann, 2009). Effective thermal insulation in buildings has an essential share of lowering the energy demand in the building sector (Coma, Pérez, Solé, Castell, & Cabeza, 2016).

Traditional insulation materials mainly consist of organic and inorganic insulation materials. The high thermal insulation performance is mainly seen on organic insulation materials; however, they have low fire resistance performance. In contrast, inorganic insulation materials show desired fire resistance; however, having low thermal insulation performance. Considering that the thermal conductivity of water is at an undesirable high level, inorganic materials will show even higher thermal conductivity in a humid environment (Jia, Li, Liu, & Jing, 2018). Therefore, studies were conducted to increase the behavior of inorganic insulation materials such as expanded perlite and glass wool.

The emergence of aerogel, which has a 3D solid network with prominent properties, pioneer the use of a combination of this material with traditional insulation materials. Aerogel is the lightest material with low thermal conductivity; hence, the availability of this material in various forms provides widespread usage of it (Koebel, Rigacci, & Achard, 2012). On the other hand, the fragility of aerogel and high production expenditure cause an adverse effect on the proliferation of the usage on construction (Jia et al., 2018). To solve these problems, the synthesis of aerogel with a reasonable cost and combine its outstanding properties with other insulation materials as composite is the contemporary approach in aerogel studies (Stefanidou & Pachta, 2020).

1.1. Aim and Scope of the Research

This research aims to produce an aerogel-modified expanded perlite and clay board (AEP/C) and investigate the physical and mechanical properties of the board. The production of the board requires the synthesis of aerogel-modified expanded perlite. A sol-gel method is chosen to synthesize aerogel-modified expanded perlite due to its flexibility to manage the process steps and control variables in steps and its allowance to low-cost synthesis.

This study consists of three parts. The first part focuses on optimizing the sol-gel synthesis of aerogel. The second part is the application of the aerogel synthesis process on expanded perlite aggregate (EPA). This application is called aerogel-modified expanded perlite (AEP), which means filling the pores and covering the surface of perlite with the aerogel. In this process, the amount of EPA is optimized. The third part of the study is concerned with preparing AEP composite with a clay matrix and presenting the physical and mechanical performances of the composite boards. The characterization and tests of composite samples are carried under the applicable TS standards. Therefore, physical and mechanical performances of composite boards are presented to offer the promised installation material.

1.2. Structure of the Thesis

This thesis comprises five chapters. The first chapter is the introduction that provides the starting point of the main idea, introduces the subject of the thesis, and clarifies the objective and the content of the thesis.

The second chapter provides the current necessity and background information about three subsections. The first subsection is about building thermal insulation materials and building acoustical materials. This section explains the board or type of materials to constitute a correlation with this research. The second and third subsections focus on the EPA and Si aerogel as building materials, usage areas, mechanical and physical properties. The recent studies examining aerogel/EPA composites and the properties of the composite in the matrix are given. This section also expresses the absence of the literature that this study wants to resolve.

The third chapter presents the organization of the study, and it is divided into three parts. The first part begins with the sol-gel method for aerogel synthesis that presents the definition, steps, and significant variables. The second part focuses on preparing and characterizing aerogel-modified expanded perlite aggregate (AEP). Then, the experimental setup and tests for AEP

characterization are defined and explained. The third part concentrates on preparing and characterizing aerogel-modified expanded perlite aggregate and clay (AEP/C) composite. Then, the characterization and tests are depicted under TS standards in the subsections.

The fourth chapter explains the results and discussion of the research, which is separated into three parts. The first part presents the optimization of the aerogel synthesis. The second part explains AEP production and the influences of parameters in steps. The characterization results and the scientific explanation behind the results are discussed. The third part focuses on the characterization of the AEP/C and the findings discussed by required values in the standards comparatively.

CHAPTER II

LITERATURE REVIEW

2.1. Building Thermal Insulation Materials

Thermal insulation in buildings enables the conservation of energy and natural sources. The reduced energy need for operation in all seasons and lowering the initial cost of the HVAC system bring about a noteworthy contribution to lowering capital expenditure of the building construction (Al-Homoud, 2005; Xu, Zhang, Lin, Di, & Yang, 2005). The dependence on the electrical and mechanical systems for thermal comfort in buildings is attenuated by thermal insulation. The energy savings in buildings are also prominent in environmental conservation (Ingrao, Messineo, Beltramo, Yigitcanlar, & Ioppolo, 2018). The diminished energy needs ensure the availability of energy for others, the ascending rate of

need for power generating plants, restraining the pollution, and the transfer of resources to future generations (Aditya et al., 2017; Al-Homoud, 2005).

There are many building thermal insulation materials which are generally accepted as basic materials and composites. These are classified in accordance with their composition: inorganic materials, organic materials, combined materials, and new technology materials (Papadopoulos, 2005). Thermal insulation materials are fabricated in several primary types as mineral blankets (polyethylene, rock wool), boards (perlite, vermiculite), loose-fillers spray foam (fiberglass, rock wool, perlite, vermiculite, cellulose), reflective materials (aluminum foil), etc. (Aditya et al., 2017; Al-Homoud, 2005). Performance attributes (durability, heat transfer mode, etc.), availability, handling, adaptability, ease of installation, and cost of building insulation materials are all essential factors for selecting the form of the material (Aditya, 2017; Papadopoulos, 2005).

The energy efficiency is evaluated with the amount of energy needed for heating and cooling a building. The thermal comfort of a building is defined by how well the building structure is controlled thermally. (Dongmei, Mingyin, Himing, & Zhongping, 2012). The thermal characteristics of the materials used in the buildings determine the building envelope's thermal efficiency (Al-Homoud, 2005). Although the insulation is ensured with these thermal blocks, materials serve a specific role with their function, form, and composition (Aditya et al.,

2017). Studies point out that effective insulation is obtained by using the insulation layer, particularly on the outer side of the wall (Ciampi, Leccese, & Tuoni, 2003; Stazi, Tomassoni, Vegliò, & Perna, 2011; Tsilingiris, 2006). According to the thermal insulation selection procedure, the efficiency and economic value of the material are evaluated immediately after the location selection (Al-Hamoud, 2005).

Rigid boards are widely used in construction due to their insulation advantages, handling, availability, ease in application processes on walls, roof, or floor systems, and low production expenditure. The application process depends on assembling and fixing panels with screws without any wet treatment. The quick install avoids moisture loss and damage to the building shell (Al-Homoud, 2005). Expanded Polystyrene (EPS) is widely preferred as an insulated panel for floors, walls, and facades due to its energy efficiency, durability, and indoor environmental quality (Sulong, 2019). EPS is produced by the spherical-shaped pellets of polystyrene and the help of a foaming agent. It has an open pore, rigid and lightweight form that enables high insulation properties. The thermal conductivity (λ) of EPS is 0.030-0.040 W/m·K (Abu-Jdayil, Mourad, Hittini, Hassan, & Hameedi, 2019). Besides having economic production, EPS is easily pliable in production and suitable for a specific application. It possesses long life and low maintenance while having high impact resistance. The required mechanical strength for the application area determines the compressive strength of the EPS via its flexible production capacity depending on the molding

geometry and process conditions (Doroudiani & Kortschot, 2003). It also allows to be sandwiched between rigid boards, and the mechanical performance of EPS is increased besides stunning insulation properties. On the other hand, EPS has a low melting point and ignites about 490 °C, and the maximum service temperature of the EPS board is 100 °C (Aditya et al., 2017). Its cell structure allows pores that store air and that causes explosion during flashover (Doroudiani & Omidian, 2010). In addition, combustible and toxic gases are released during the explosion (Stec & Hull, 2011). The flame-retardant modification is needed to reduce the easily flammable characteristic of EPS.

2.2. Expanded Perlite Aggregate as Building Material

2.2.1. Definition and the Usage Areas of Expanded Perlite Aggregate as a Building Material

The name "perlite" is a derivation from "perlstein," and meaning glassy rocks with numerous concentric cracks, which resemble broken pearls (Doğan & Alkan, 2004). The petrological definition of perlite is a volcanic glass which has strain behavior to cooling process lead to "onion" structure of fracturing. This form is also well-known as perlitic structure (Otis, 1960). It is a glassy volcanic rock composed mainly of SiO_2 and Al_2O_3 and lesser amounts of several metal oxides

(Alkan & Doğan, 2001). Chemically, it is termed as metastable amorphous aluminum silicate (Doğan & Alkan, 2004).

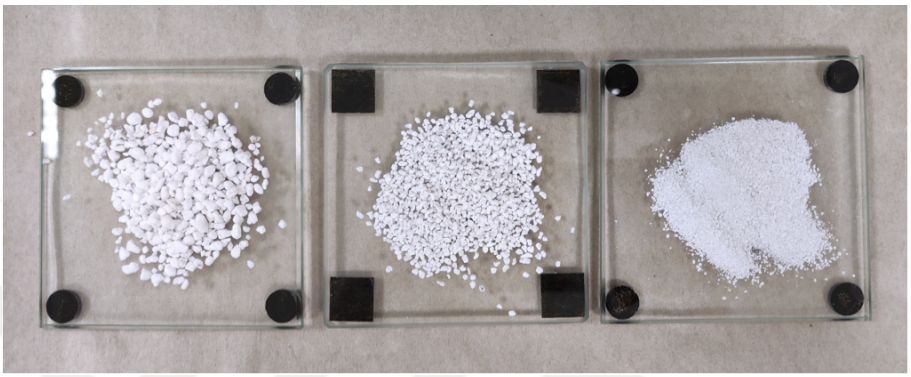

Figure 1 EP with different grain sizes (photographed by the author)

Perlites that have been ground, resized, and extended at softening temperatures are known as expanded perlite (Otis, 1960). It also contains 2-5 wt% water, enabling it to expand while heating to its softening temperature. The water in perlite grains is vaporized under heating temperatures of 700-1200°, and perlite can be extended to a volume of up to 15-20 times its initial size (Taherishargh, Belova, Murch, & Fiedler, 2014). According to Mineral Commodity Summaries (U.S. Geological Survey, 2021), the principal perlite-producing countries are China, Greece, Turkey, and the United States in descending order of production.

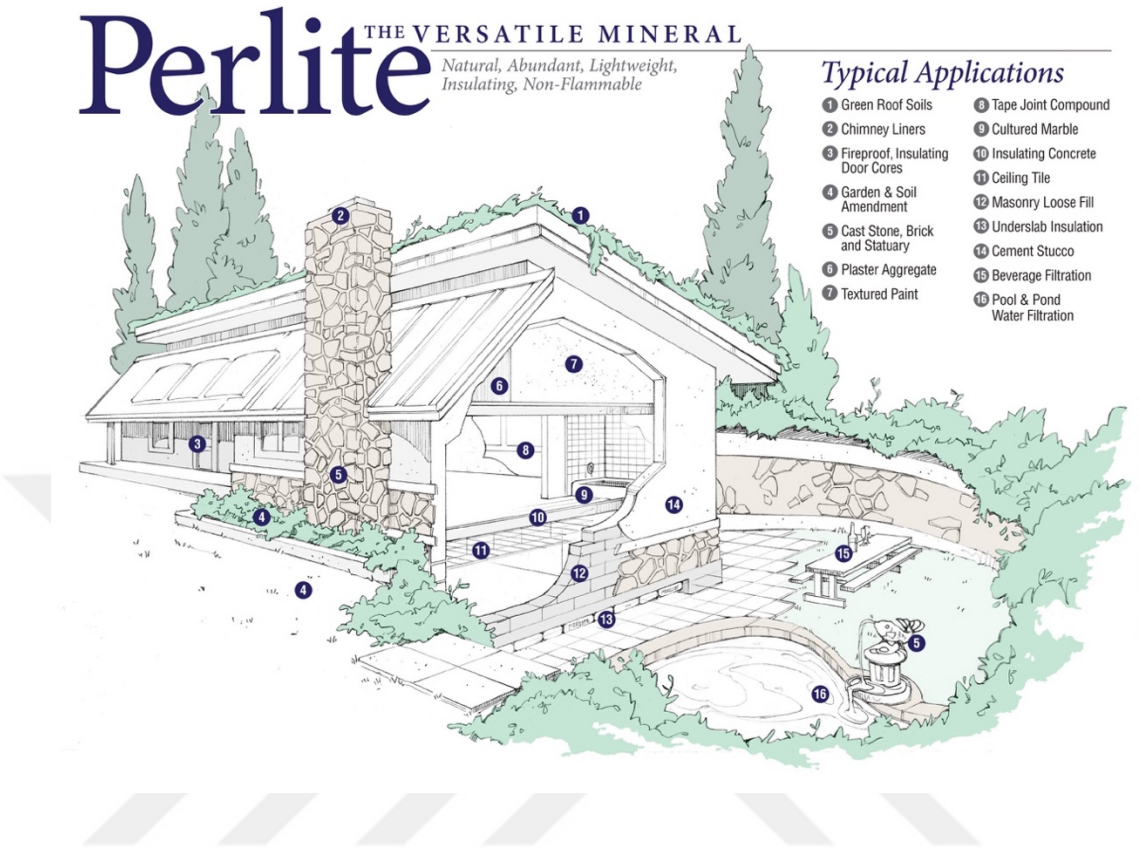

Figure 2 Typical applications of perlite mainly in construction (Taken from www.perlite.org)

Expanded perlite aggregate offers attractive properties for commercial applications; desired thermal and acoustic properties, low bulk density with high surface area, chemical inertness, fire resistance, and water retention (Ciullo, 1996; Ennis, 2011). EPA has been broadly used in horticulture, industry, and construction (Haery, 2017; Rashad, 2016). It can be used for filtration of chemical and water products, industrial effluents, pharmaceuticals, combating oil spillage, filler in textured paints, filter aid in the processing of foods in the industry; used for aeration and drainage of the soil, rooting medium, carrier for fertilizer, additive

in animal feeds in horticulture (Ciullo, 1996; Roulia, Chassapis, Fotinopoulos, Savvidis, & Katakis, 2003; Singh & Garg, 1991).

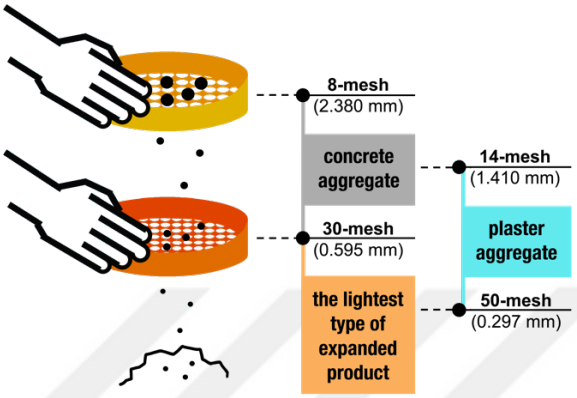

Figure 3 The mesh size ranges for different applications (Information is taken from Haery (2017) and Johnstone & Johnstone (1961), and the image is drawn by the author)

Expanded perlite aggregate is a prominent construction material with its thermal and acoustic insulation performance and substantial particle size range. As shown in Figure 2, it is used as an aggregate in mortar, plaster, brick or concrete type of building materials, for example, as loose-fill insulation in building cavities, wallboard, lightweight fire-resistant coatings, lightweight concrete (Austin & Barker, 1998; Ciullo, 1996; Singh & Garg, 1991). Generally, different mesh size ranges are suitable for specific applications (Haery, 2017). The size of perlite particles preferred for the lightest types of expanded product, concrete or plaster aggregate, is shown in Figure 3. Current applications are fronted on composites to upgrade the materials' physical, mechanical, and acoustic properties via EPA

substitution/addition in cementitious materials, using EPA as media for polymers or binders (Rashad, 2016).

2.2.2. Physical and Mechanical Properties of Expanded Perlite Aggregate

Expanded perlite aggregate has from bright greyish to snowy white color depending on the reflectivity of light inside the cellular structure (Singh & Garg, 1991). It is a porous, lightweight, chemically inert, fire-resistant material having thermal and sound insulation properties. The physical properties of this material will be examined depending on their relevance with these titles.

2.2.2.1. Porosity

Porosity is the fraction of the void volume to the overall volume of the material's mass. The porous structure supplies high volumetric and surface absorption capacity to EPA and enables the application of EPA on aeration and drainage of the soil, carrier for fertilizer, odor capture in manure or moisture-retaining (Afshari et al., 2011; Ciullo, 1996). Vesicular texture in volcanic rocks is cavities formed by the expansion of gas bubbles while the solidification of the rock occurs (Zou et al., 2013). Nevertheless, pore size determines the application of the material which is used. For example, narrow pore size distribution is suitable for filtration

application, whilst large pores transport reactants between channels. In materials science, several applications tend to use high porous materials in order to utilize a large surface area (Chan & Brownsten, 1991). Therefore, porosity, pore size, and pore geometry determine the nature of the materials (Ishizaki, Komarneni, & Nanko, 2013). The cellular structure and closed cells of the EPA provide progressive crushing characteristics that enable the maintenance of the cellular structure of the perlite-reinforced material for longer service life. Conversely, high porosity levels decrease the mechanical strength of the material (Haery, 2017). The porous structure of EPA is demonstrated in Figure 4.

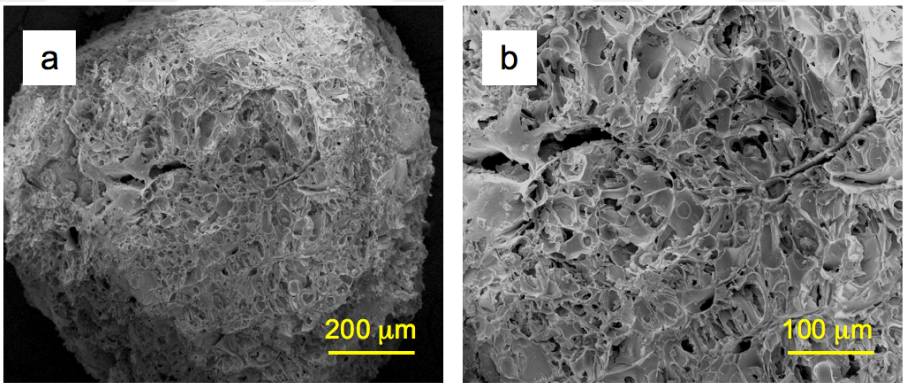

Figure 4 Scanning electron microscope (SEM) image of (a) exterior and (b) cross-section of EPA (Images taken by FEI Scanning Electron Microscope in National Nanotechnology Research Center (UNAM))

2.2.2.2. Density

Compared to normal-weight aggregates, lightweight aggregates are lighter depending on their porous nature. The specific weight and density of EPA varies according to the pore distribution, pore sizes, and expansion rate. According to Ishizaki et al. (2013), augmentation of the porosity level decreases the density and increases the specific surface area of the material. The low density allows the application of EPA in loose-fill insulation in cavity walls, for filling cores, the air holes of masonry blocks, in lightweight concretes and plasters. It helps lower the destructive effects of earthquakes by reducing the unit weight of high buildings (Ahmed, 2015).

2.2.2.3. Water Absorption

Expanded perlite aggregate has a uniformly distributed microvesicular texture that allows water molecules to vaporize quickly from pores while a small degree of expansion occurs (Haery, 2017). On the other hand, the inclusion of water into pores of EPA causes the increase of heat conductivity, therefore undesirable thermal insulation properties (Topçu & Işıkdağ, 2007). Therefore, the water absorption capacity test is significant for the material to analyze the suitability of the construction, and this capacity gives information about boards' open porosity.

2.2.2.4. Acoustic and Thermal Insulation Properties

Morphologically, closed porous materials are generally used for thermal and sound insulation purposes (Ishizaki et al., 2013). EPA is classified as a closed porous material, has low thermal conductivity and high sound absorption performance. Also, its surface has unlinked open pores that provide a cavity resonance structure for sound absorption. Therefore, EPA is used in various forms such as mortar or plaster with mixing binders such as cement and gypsum with other insulation materials to enhance the sound insulation and thermal behavior (Rashad, 2016). The thermal resistance and thermal conductivity of EPA board products are determined in accordance with EN 12667 or EN 12939 standards.

2.2.2.5. Chemical Inertness

Expanded perlite aggregate cannot be involved in chemical reactions depending on its chemical stability and maintains its original properties after exposure to chemical reagents. It dissolves slightly in weak acids and moderately in NaOH (Singh & Garg, 1991). Therefore, it is used in applications needing moisture retardancy or exposing chemical, bacterial environment for extended periods (Roulia et al., 2003; Taherishargh et al., 2014).

Table 1 Typical physical properties of EPA (Information is taken from Rashad, 2016; Singh & Garg, 1991; Topçu & Işıkdağ, 2008, and prepared by the author)

Color	White
Bulk density (loose)	32 – 400 kg/m^3
Unit weight	2.2 – 2.4 g/cm^3
Softening point	871 – 1093 °C
Melting point	1260 – 1343 °C
Specific heat	387 J/kg·K
Thermal conductivity at 24 °C	0.04 – 0.06 W/m·K
Sound insulation	18 db (125 Hz)
pH (of mud water)	6.5 – 8
% Retention of water	35 – 50

2.2.2.6. Fire Resistance

EPA is an inorganic compound containing tightly bonded atoms with an ionic bond to its molecules. Therefore, this inorganic material cannot ignite in the presence of oxygen; therefore, it is non-combustible. EPA is not destroyed under temperatures; its softening point is also used to protect other construction elements from failure in rapidly rising temperatures. For example, EPA is used as composite or aggregate filler for sprayed on fire protection coatings and plasters and provides insulation of structural steel from fire conditions (Kusiorowski,

Witek, Majchrowicz, Kleta, & Jirsa-Ociepa, 2019). Therefore, its inorganic structure is more favorable than organic materials for use as building materials. Typical physical properties of EPA are given Table 1. The reaction to fire of the EPA products is determined by TS EN 13501-1 standard.

2.2.3. Recent Studies of Expanded Perlite Aggregate

Expanded perlite aggregate was subjected to wide-extend studies, especially as material for enhancement of properties of a material (Rashad, 2016). Most studies with EPA-containing building materials gave at least two physical or mechanical properties comparatively (Jedidi, Benjeddon, & Soussi, 2015; Sengul Azizi, Karaosmanoglu, & Tasdemir, 2011; Türkmen & Kantarcı, 2007). The inclusion of EPA in cementitious materials pointed to the reduction of unit weight of the mixture (Dawood, 2015; Lanzón & García, 2008). The porous structure of EPA in the mixture led to a decrease in the unit weight and density, thus using EPA for the production of lightweight mortar, concrete, plaster, brick, etc (Binici & Kalayci, 2015; Maaloufa, Mounir, Khabbazi, Kettar, & Khaldoun, 2015). Moreover, the substitution of EPA in a mixture caused the reduction in the mechanical strength of mortars, bricks, and plasters, and also thermal conductivity could be decreased by the inclusion of EPA (Işıkdağ, Topçu, & Gökbel, 2015; Yıldızel, 2018). Reduction in the ratio of EPA in the mixture

indicated the need for additives such as silica fume, gypsum, colemanite, aerogel to enhance the matrix's mechanical properties.

Recent research is on mixing ratio optimization of a porous thermal insulation board was conducted by Yılmazer & Baytekin (2017). The authors aimed to optimize the mixing ratios for analyzing the thermal resistance performance of clay-based expanded perlite board. The critical approach in the study was keeping the Unit Volume Mass (UWM) ratio low for the thermal resistance of a material. EPA has a low unit weight volume intrinsically; hence it was used as porous material in the study. Additionally, to increase the strength and elasticity of the board with binding properties, rock wool was used. The rock wool addition and pre-process to bind them could not help to reach the target values. One of the essential outputs of this study was that the silanized material had a negative effect on the mechanical strength of the composite as it would reduce the ionic bonding while preparing the composite.

Another study was carried for the chemical synthesis and process optimization of a porous thermal insulation board (Yilmazer, 2019). The clay and perlite ratios and chemical processes used in this study were different from the previous study. Rock wool and glass fiber were used for composite reinforcement. As a result of this research, the target limit values could not be reached. More significantly, EPA was sintered (shrinking and turning into a glassy form) while

being processed in the composite, and its density was increased although the chemical pretreatment was applied to the particle skin. As we know, the thermal conductivity increases proportionally with density. The increment in the density increased compressive strength, thus the mechanical performance of the composite. The significant outputs of this study are the determination of the ratio of clay and perlite forming the composite and examining the physical and mechanical property values. For example, the study showed that bending strength of 0.52 N/mm^2 could be reached as a board made of clay-based expanded perlite. Additionally, glass fiber and rock wool reinforcement helped to reach 3.7 N/mm^2 bending strength. On the other hand, the study revealed that the composite needs additional material or process application to obtain composite with desired thermal and mechanical performance.

Expanded perlite aggregate is an excellent thermal insulation material due to the low conductivity of the air in its pores (Yılmazer & Baytekin, 2017). Along with this material, other materials to reinforce the clay matrix should also be lightweight and have low thermal conductivity. Materials with both high mechanical performance and low thermal conductivity are a priority for studies with board production. According to the findings of these studies, using a filler material with better thermal performance inside the EPA would be beneficial. The aerogel is a promising candidate with its high thermal insulation performance the low density (Sarawade, Kim, Kim, & Kim, 2007; Riffat & Qiu, 2013).

2.3. Silica (Si) Aerogel and Architectural Application

2.3.1. Definition and Properties of Silica Aerogels

An amorphous solid substance with a three-dimensional network is a silica aerogel (Pierre & Rigacci, 2011). Its name is derived from the gel production method (Fricke & Tillotson 1997). It is frequently manufactured in industry, and research is being performed to improve the qualities of silica aerogels in order to boost production; because silica is a widespread resource and has a stable structure. Si aerogel has a pore volume of 80 to 99.8% of its volume and a density of 0.003-0.5 g cm^{-3} (Begum et al., 2021). Regarding porosity, pore diameters of Si aerogels range between 5 and 100 nanometers. The synthesizing methods specify the pore sizes and texture and the characteristics of aerogels depending on the porous network (Hüsing & Schubert, 1998).

2.3.1.1. Optical Property of Silica Aerogels

The visible light transmittance of Si aerogels is very high; therefore, most commercially used aerogels are optically transparent. They also scatter the visible light comparatively depending on the solid gel network. The gel structure

has nanometer-scale network defects that cause yellowish color by transmission and bluish color by reflection inside the gel. Hence, Si aerogels have transparent to opaque application potentials related to the usage field. The precursors that are used in the production and synthesizing method allow controlling the transparency of aerogels. The optical images of transparent and translucent Si aerogels are shown in Figure 5.

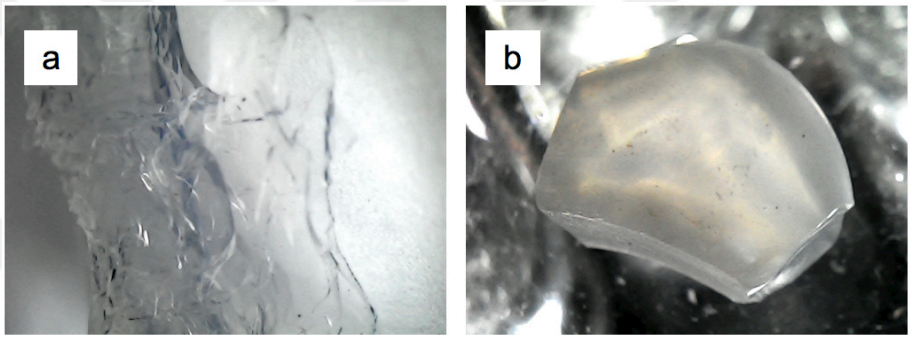

Figure 5 The optical images of (a) transparent and (b) translucent Si aerogels (Photographed by the author)

2.3.1.2. Thermal Conductivity of Silica Aerogels

The aerogel's relatively small pores restrict heat transport via conductive and convective gas transport (Koebel et al., 2012). Aerogel’s low density infers a low fraction of solid part; therefore, there is only a narrow solid pathway for heat transfer via conduction (Kanamori, 2011). Silica aerogel’s typical thermal

conductivity is around 0.015 W m^{-1} K^{-1}. Considering air's thermal conductivity, 0.026 W m^{-1} K^{-1}, and conventional insulation materials, 0.03–0.04 W m^{-1} K^{-1}, it can be expressed as Si aerogels have prominent thermal insulation properties (Koebel et al., 2012). It is widely known that they are used in space missions subjecting the sudden temperature drops.

2.3.1.3. Acoustic Property of Silica Aerogels

The acoustic properties of Si aerogels depend on the aerogel texture, pore sizes (micro-and mesopores), density, interstitial gas nature, and pressure (Pierre & Rigacci, 2011). According to Begum et al. (2021), sound dissipation is mainly related to heat transfer inside inner-grain pores and the particles. The gas phase in the environment and the rigid aerogel structure ensure the transmittance of wave energy, the attenuation of the sound is ensured in both velocity and amplitude (Burger & Fricke, 1998; Pierre & Rigacci, 2011).

2.3.1.4. Sorption Property of Silica Aerogels

Si aerogels are highly tolerant of particles and molecules on a wide scale because of their solid skeleton and high pore volume. Aerogels with various densities, pore volumes, and aerogels with different surface chemistry point out

the divergent fluid flow behaviors on aerogel surfaces and the entrapment of molecules (Buisson, Hernandez, Pierre, & Pierre, 2001). Functionalization, hybridization, and surface coating of aerogels allow designing the entrapping, delivering, and releasing behavior of aerogels and the time interval of these behaviors (Veres, López-Periago, Lázár, Saurina, & Domingo, 2015). Therefore, studies on aerogels consist of a wide range of applications that require entrapment, storage, or release. For example, medical drug release, agricultural chemical absorption, wastewater filtration, energy storage applications are common usages of Si aerogels (Stergar & Maver, 2016).

2.3.1.5. Mechanical Property of Silica Aerogels

Depending on the low density of solid porous skeleton, Si aerogels' strength values are very low (Ma, Roberts, Evost, Jullien, & Scherer, 2000). It is possible to produce aerogels with having various features. Variables can determine the properties of aerogels during synthesizing. Therefore, the strengthening of aerogels by avoiding a cracked solid network of aerogels in production is achieved by controlling parameters through synthesizing routes (Burger & Fricke, 1998). In addition, compressive strength, elastic moduli are sensitive to the environment of aerogels because of the crack formation in the structure depending on these variables (Parmenter & Milstein, 1998).

2.3.2. The Usage Areas of Silica Aerogels

As aforementioned, Si aerogels have low density with high porosity; hence, low thermal conductivity (Riffat & Qiu, 2013). Their reinforced and organic-inorganic hybrid synthesizing potentials and production opportunities with extensive pore sizes permit upgraded properties of aerogels (Mazraeh-shahi, Shoushtari, & Bahramian, 2015). These excellent properties draw attention in aerospace, electronics, chemical, biomedical applications, food-related technologies, outdoor apparel, and construction in monolith, powder or film application forms (Stergar & Maver, 2016).

Aerogels have a gradually increased market in the building industry, significantly depending on their superior insulation capabilities. For example, an aerogel incorporated thermal insulation material with 20 mm thickness leads to a 90% heat consumption decrease (Cuce, Cuce, Wood, & Riffat, 2014a; Cuce, Cuce, Wood, & Riffat, 2014b). They are installed in both exterior and interior parts of construction where space-saving is required. Therefore, the aerogel is broadly used in facades, roofs, and windows in buildings, as examples of different uses of aerogel are presented in Figure 6.

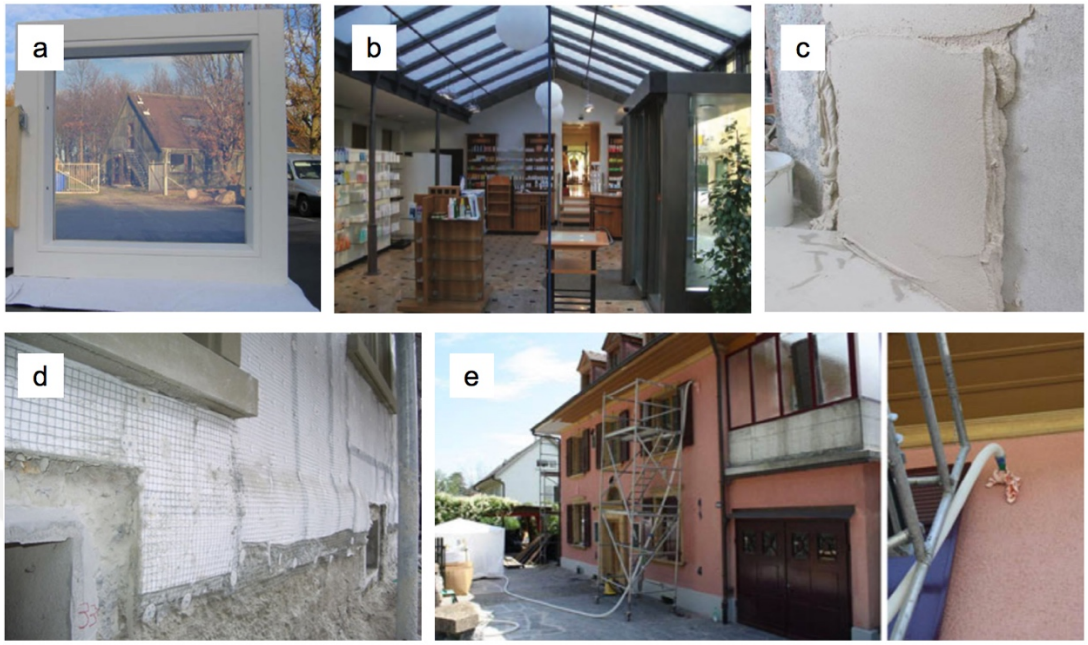

Figure 6 Photographs of (a) aerogel glazing, (b) the translucent aerogel roof, (c) render system, (d) the wall and window sill detail from the retrofit insulation with aerogel blankets, (e) the injection hole for cavity wall insulation (Koebel et al., 2012; Riffat & Qiu, 2013)

According to Koebel et al. (2012), the insulation performance of a material is evaluated considering its installation thickness, thermal conductivity, mechanical strength, and cost comparatively. Generally, thinner insulation materials are chosen in applications for space-saving; however, it has to be affordable as well as the material's thermal insulation performance has to be satisfactory. Aerogel and vacuum insulation panel (VIP) comparison is an actual example of this viewpoint. Thermal insulation of VIP is provided by evacuation of porous core material, thus the heat transportation of gas molecules inside this core. On the

other hand, aerogels need no evacuation due to their porous structure, and their thermal conductivity is lower than VIP. Nevertheless, the expenditure on aerogels is higher than VIPs; therefore, VIPs are widely preferred as insulators rather than aerogel panels. On the contrary, in some applications, the direct use of aerogel does not raise the price of the building material much but significantly reduces the strength of this material (Kim, Seo, Cha, & Kim, 2013). Consequently, aerogel's physical and mechanical problems are solved by composite production with aerogel reinforcement (Wang & Jana, 2013). Additionally, aerogel-filled composites help lower the cost of synthesis and require less time to produce than aerogels.

2.3.3. Recent Studies of Aerogel-Modified Expanded Perlite Aggregate (AEP)

Expanded perlite aggregate (EPA) is an abundant natural material and permits composite production depending on its porous nature. A promising approach in studies uses silica aerogel as a reinforced material inside the EPA (Wang, et al., 2018). In many studies, aerogel is synthesized inside the pores of EPA by adding a source material, silica, during the phases (Koebel et al., 2012; Rao & Bhagat, 2004). The disadvantage of water absorption of EPA is reduced, and the fragility problem of aerogel is overcome by the help of the skeleton of EPA (Chen et al., 2020).

The aerogel synthesis method is the most influential factor in production expenditure and controlling the variables in the process. Generally, a sol-gel method is chosen to synthesize aerogel-modified expanded perlite due to the flexibility to manage the process steps and control variables in steps. The method also permits synthesizing the aerogel at ambient pressure, which significantly reduces the synthesis cost. The synthesis steps of aerogel/EPA composite have significant parameters that determine the features of the end product. If we focus on the studies synthesizing aerogel using the sol-gel method and under ambient pressure, we come across aerogels with different properties obtained by changing the process parameters. Studies are widely focused on optimizing and controlling variables and synthesizing the Si aerogel/expanded perlite composite with low thermal conductivity and low cost. Peng & Yang (2013) studied the surface characteristics of aerogel-modified EPA composite. The surface area of EPA was 15 m^2/g, while the aerogel-modified expanded perlite aggregate was 196 m^2/g. The aerogel-modified EPA's thermal conductivity was 0.063 W m^{-1} $K^{-}1$ by a 13.3% decrease of EPA's thermal conductivity. Jia et al. (2018) studied important variables on synthesis steps and presented effects on an experimental scale. The pore, volume, and property correlation were discussed with the microstructure of the composite. The results showed that aerogel causes a decrease with a 14.7-31.8% in thermal conductivity of the composite. Wang et al. (2018) developed a recipe determining the time and reagent ratios for synthesizing aerogel/EPA composite. The results demonstrated

that the aerogel addition has no significant change in the thermal conductivity of EPA.

The direct use of aerogel-modified expanded perlite in buildings does not seem possible due to the inability to reach the target limit values or allow mass production. For this reason, research was commonly concentrated on studying the physical and mechanical properties of aerogel-modified expanded perlite embedded into a matrix. The problem of low mechanical strength and high cost of aerogel-based building materials have been solved by Si aerogel/EPA composite reinforcement on different materials. The influence of aerogel/EPA substitution on the mechanical behaviors of fly ash-based lightweight wall material (LWM) and Si aerogel/EPA composite was investigated (Chen et al., 2020). The results revealed that the increment of aerogel/EPA composite amount causes decreasing the compressive strength. Wang et al. (2018) examined the performance of concrete prepared by aerogel-filled EPA addition. Both the mechanical strength and the thermal conductivity of the concrete decreased while the aerogel-filled EPA amount increased. Recently, Jia & Li (2021) studied the mechanical behavior of cement-based aerogel/EPA composite. The compressive strengths of composites were between 3.79 and 14.47 MPa.

Consequently, the typical approach of studies carrying out to date is that aerogel/EPA composite for producing thermal insulation material is adequate for

low-cost applications. Despite the studies on aerogel-filled EPA composite substitution on several but mainly cementitious materials, the alkali-silica reaction (ASR) is the origin of deterioration in concrete over time. For example, clay has no side effects such as ASR and is a low-cost material as matrix/binder in composites (Yılmazer & Baytekin, 2017). As mentioned in *Section 2.2.3*, Yilmazer (2019) investigated the thermal and mechanical properties of rock wool reinforced clay-based expanded perlite board. However, the effects of aerogel addition were not investigated in the previous research. In addition, no study of aerogel/EPA board sank into clay matrix has been found in the literature. This study aims to cope with this absence in the literature. Therefore, this study will be the pioneer to investigate aerogel/EPA board properties with a clay matrix.

2.3.4. Sol-Gel Method for Aerogel Synthesis

Sol-gel is a two-step synthesis method that transforms dispersed solid particles (monomers) into an integrated solid network. The particles in a colloidal solution (sol) acts as precursor molecules for the aerogel network. These molecules undergo a polymerization process in a liquid reaction medium and establish a three-dimensional gel network (Pierre & Rigacci, 2011). The sol-gel method was used for both aerogel synthesis and aerogel-modified expanded perlite synthesis. The process of the sol-gel method is illustrated in Figure 7.

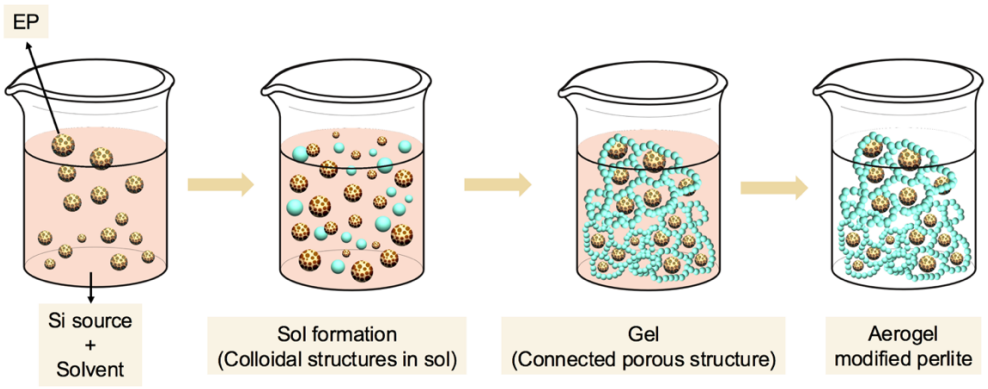

Figure 7 Schematic of sol-gel synthesis (illustrated by the author)

The two-step sol-gel process allows controlling the hydrolysis and condensation reaction rates (Kim, Chakrabarti, Oh, & Whang, 2003). There are oxalic acid and ammonia base catalysts are used in the process. The catalyst is the chemical agent that increases the rate of reactions without undergoing any permanent chemical change and participates in reactions to form the end product. The significant reactions are *hydrolysis* and *condensation* in the sol-gel method (Figure 8). These reactions are performed by the presence of acid and base catalysts.

TEOS, Si source, is hydrolyzed in the acid catalyst and the water (H_2O). Then, these hydrolyzed species ($Si(OH)_4 + 4C_2H_5OH$) undergo condensation with the help of a base catalyst (ammonia, NH_4OH). The concentration (molarity, M) of the base catalyst is vital to determine the gelation time; therefore, the properties of the gel. The instantaneous gelation and cracks over the surface of the gel are

observed in the high concentration of the catalyst. Moreover, the lack of the base catalyst causes a longer gelation duration (Rao & Bhagat, 2004). Condensation reactions form a SiO_2 solid matrix (Brinker & Scherer, 1990). The hydrolysis and condensation reactions are given in the following equations in Figure 8.

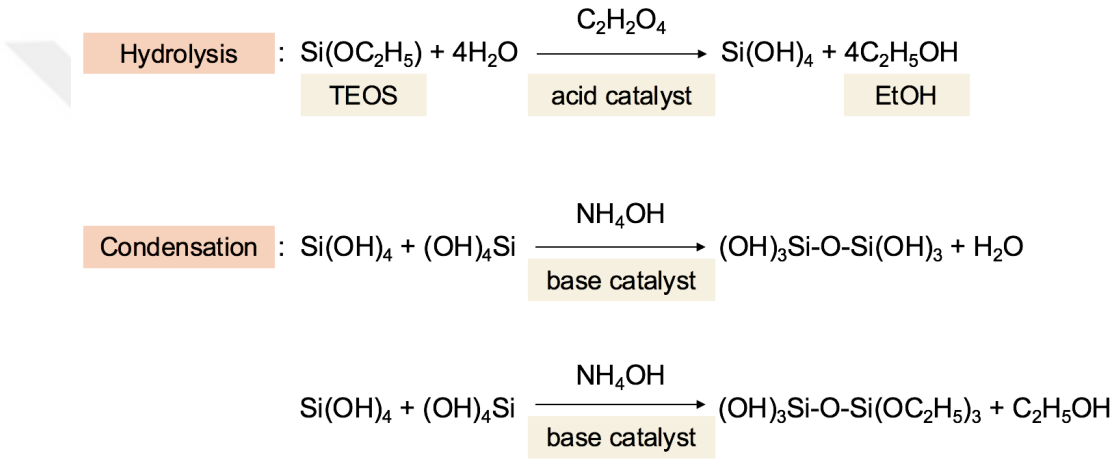

Figure 8 Hydrolysis and condensation reactions

Hydrolysis and condensation reactions lead to the aging and drying processes. The aging process yields a stable gel structure after a specific time by exchanging products in the pores of aerogel. In this step, EtOH has a significant role in synthesizing the uniform aerogel by slowing the reaction rate and preserving the structure of the gel during the surface exchange (Shi, Wang, & Liu, 2006). Then, n-hexane and TMCS are used for surface modification. TMCS has violent reactions with the water inside the silica gel, attaching the network of the gel and converting Si-OH bonds into Si-CH_3 (Wang et al., 2018). On the other

hand, n-hexane availability slows down the reaction and provides homogeneous surface modification. The duration of waiting for the gel in the EtOH, n-hexane, and TMCS is crucial for the aerogel structure. The long waiting in EtOH causes high surface tension on the gel and structural collapse in this step. Also, a high amount of TMCS and long duration causes breaks on the gel, and insufficient waiting duration leads the incomplete reaction. The solvent exchange and surface modification steps prohibit the shrinkage of the gel in the drying process (Wu, Yu, Cheng, & Zhang, 2011). The drying process is designed to remove excess EtOH and water from the pores of the gel without disturbing it. This process is carried by gradually increased heat treatment at ambient pressure to form a continuous structured aerogel (Dorcheh & Abbasi, 2008; Sarawade et al., 2007).

The sol-gel method is adopted to constitute aerogel structures into pores and the surface of EPA. The silicic acid is constituted into the pores of EPA by hydrolysis of Si source in the presence of acid catalyst and H_2O. With the addition of a base catalyst, condensation reactions take place. The aging process is carried to obtain a well-constructed gel structure by surface modification of aerogel. The drying process removes the excess solvent from the pores of aerogel and EPA, and aerogel-modified expanded perlite aggregate (AEP) is obtained. How the aerogel fills the perlite pores and covers the perlite is illustrated in Figure 9.

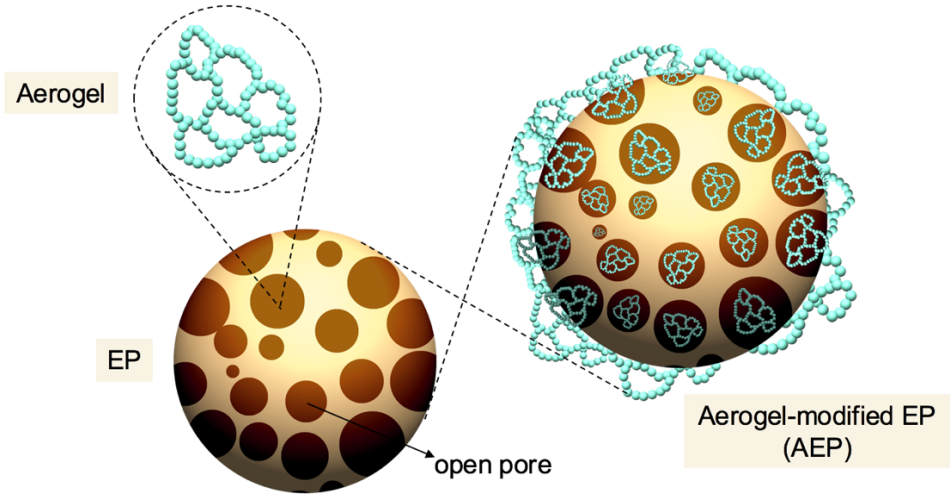

Figure 9 The representation of AEP. Inspired from the schematic diagram of Jia et al. (2018) (modified and drawn by the author)

CHAPTER III

EXPERIMENTAL STUDY

3.1. Design of the Research

This study aims to produce an aerogel-modified expanded perlite and clay board and investigate the physical and mechanical features of the board. In order to achieve this goal, optimization of the aerogel synthesis and then optimization of the aerogel-modified expanded perlite (AEP) synthesis is required. The aerogel-modified particles obtained are used in aerogel-modified expanded perlite and clay board (AEP/C) production. For this purpose, aerogel synthesis, aerogel-modified expanded perlite synthesis, and the production of aerogel-modified expanded perlite and clay board were discussed, respectively. Therefore, it can be said that this study consisted of three consecutive parts.

1. *The optimization of aerogel synthesis*

A two-step acid-base catalyzed sol-gel method was used for synthesis in the first part. Previous studies were considered for the amounts and ratios of chemicals and duration of a process used in this method (Hilonga, Kim, Sarawade, & Kim, 2009; Rao & Bhagat, 2004; Sarawade et al., 2007). Aerogel synthesis was tried with these amounts and rates; however, the synthesis was not successful. For this reason, the need for optimization arose. Optimization covered variables that are effective in the success of the synthesis; the amounts and concentrations of catalysts. The concentration of the acid catalyst is changed in a controlled manner, and its effects are observed. When the appropriate result is observed, the amount of base catalyst is studied systematically. After stages are completed in this way, an optimized recipe for the aerogel synthesis is formed.

2. *The optimization of the aerogel modification of expanded perlite aggregate*

The sol-gel method was used for synthesis in the second part. The optimization is attained by determining the amount of expanded perlite aggregate required for the optimized recipe in the first operation. The perlite amount is increased in a controlled manner, and its effects are observed. The microstructural analysis of particles was examined by scanning electron microscope (SEM) images. With the optimized

expanded perlite aggregate amount, the aerogel-modified expanded perlite production recipe is obtained. This recipe produces the particles is used for the third part of the study.

3. *The production of aerogel-modified expanded perlite and clay board*

The boards were produced by following the optimized synthesis process of the previous study (Yılmazer, 2018). *Microstructural analysis of the boards* was investigated, their *unit volume mass (UVM), specific gravity (SG), water absorption capacity, and bending strength* values were measured according to applicable TS standards. The parts of the synthesis are illustrated in Figure 10.

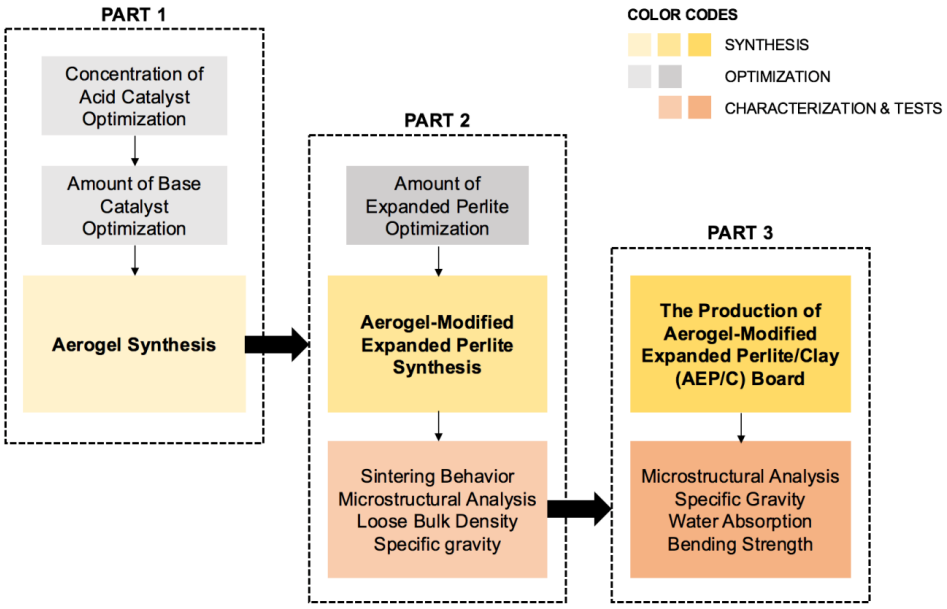

Figure 10 The flow chart of the design of the study

3.1.1. Research Question

The research question of this thesis is as follows:

- What is the effect of aerogel modification on mechanical behaviors of a thermal insulation board made of clay-based EPA?

3.1.2. Hypothesis

The hypothesis of this thesis is as follows:

- There is a contribution to the mechanical strength of clay-based aerogel-modified EPA board.

3.2. Instruments and Materials

Experiments were conducted in the Innovative and Smart Building Materials Laboratory in the National Nanotechnology Research Center (UNAM). The Nüve dry air sterilizer oven, Nüve muffle furnace, and precision balance were used in experiments in all parts. These devices are shown in Figure 11. 500 ml and 1000 ml of beakers; 50 ml and 100 ml of graduated cylinders, glass pipettes, metal

spoons, molds with pistons, and a vessel were used. The photograph of this equipment is given in Figure 12.

Figure 11 The photos of (a) Nüve muffle furnace (left) and Nüve dry air sterilizer oven (right), (b) precision balance and (c) vibrator

The following chemicals and materials were used for the synthesis of aerogel: Tetraethyl orthosilicate, (TEOS, $Si(OC_2H_5)$) as a Si source, oxalic acid dihydrate ($C_2H_6O_6$) and ammonia (NH_4OH) were used as acid and base catalysts,

respectively. Ethanol (EtOH, CH_3CH_2OH), distilled water (DH_2O), and n-hexane (C_6H_{14}) and trimethylchlorosilane (TMCS, $(CH_3)_3$ SiCl) were other reagents. The brands and degree of purity of chemicals are namely, as follows: TEOS (for synthesis Merck, ≥ 99.0% (a/a)), $C_2H_2O_4$ (Merck, 99.5-102.0%), EtOH (absolute for analysis, Merck), n-hexane (Merck) and TMCS (Merck). The chemicals above and expanded perlite aggregate with <3mm particle size (Persan Perlite A. Ş.) were used for aerogel-modified expanded perlite synthesis.

Figure 12 At the back side, from left to right; the photo of molds with piston, 50 ml and 100 ml of graduated cylinders, 1000 ml of beaker. In the front side, from left to right; a wooden mold, vessel (with purple color), glass pipettes and spoons

Expanded perlite aggregate and ready-made clay (Güray Seramik A.Ş., Avanos, Nevşehir) were used for the control group of the board production. The chemical composition of clay and perlite is given in Table 2. The synthesized aerogel-modified expanded perlite and clay were used for aerogel-modified expanded perlite/clay boards. Wooden molds were used in addition to the equipment given above. The vibrator was used with the other devices.

Table 2 The chemical contents of the perlite and the clay (Öztürk, 2017; Yilmazer, 2019)

Chemical Contents	Composition Perlite (%)	Composition Clay (%)
SiO_2	71.0 – 75.0	56.29
AlO_3	12.5 – 18.0	14.62
NaO_3	2.9 – 4.0	
K_2O	0.5 – 5.0	3.25
CaO	0.5 – 0.2	13.33
Fe_2O_3	0.1 – 1.5	7.02
MgO	0.2 – 0.5	2.86
TiO_2	0.03 -0.2	0.74
MnO	0.0 – 0.1	0.19
SO_3	0.0 – 0.2	0.11
FeO	0.0 – 0.1	
Cr	0.0 – 0.1	
Ba	0.0 – 0.05	
PbO	0.0 – 0.3	
Na_2O		1.06

3.3. Experimental Study

3.3.1. Part 1: Aerogel Synthesis

The two-step acid-base catalyzed sol-gel preparation procedure of the aerogel synthesis is described below.

25 ml TEOS and 125 ml EtOH were measured in graduated cylinders and then poured into the 500 ml beaker. Then, 10 ml of oxalic acid catalyst was measured with the glass pipette and was added to the solution, and the beaker was sealed and stirred by hand for 30 min. The beaker was left on a flat surface. After 24 hours, 5 ml of ammonia base catalyst was added to the solution dropwise with the glass pipette while the beaker was stirring by hand. The solution was transferred to the molds with a piston, and the caps were covered. After a day, the gelation occurred. The gel was removed with the help of pistons and transferred into the beaker containing EtOH. The gels were waited in EtOH for 6 hours and then in n-hexane/TMCS (5:1 V/V) for 24 hours (aging step). Samples were exposed to heat treatment of 60 °C for 4 hours, 80 °C for 2 hours, 120 °C for 2 hours, and 200 °C for an hour in Nüve muffle furnace (drying step). The flowchart of the aerogel synthesis is given in Figure 13 (left).

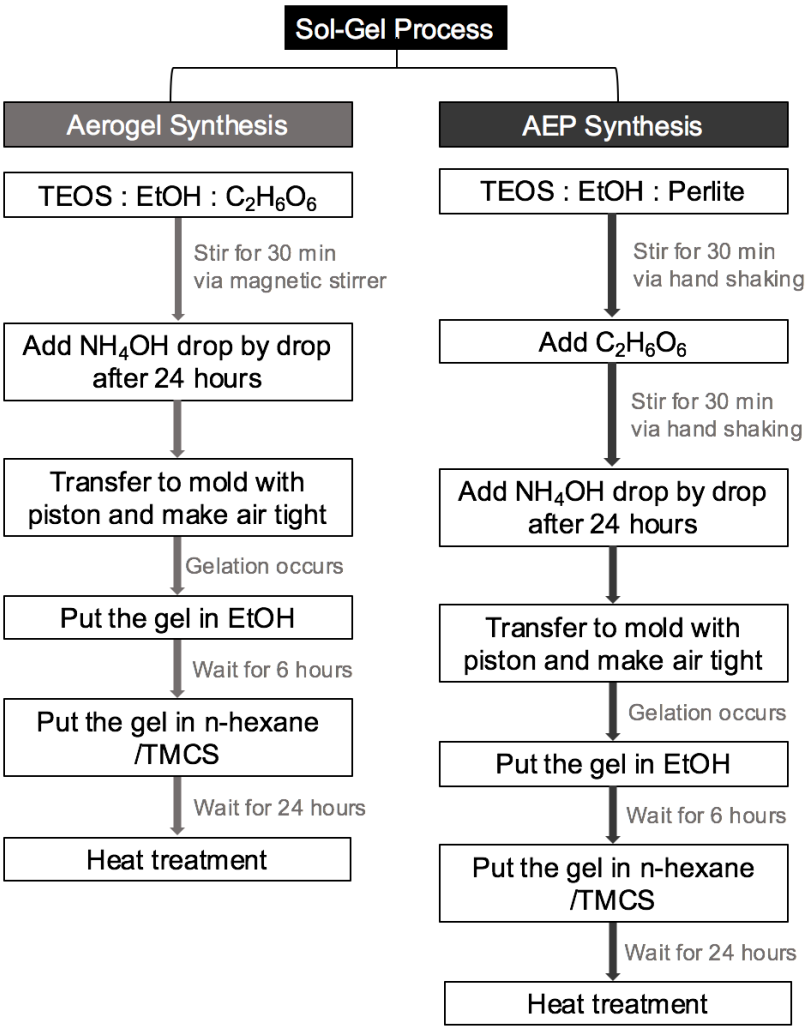

Figure 13 The flow chart of preparation of silica aerogel (left) and silica aerogel-modified perlite, AEP (right)

As stated previously, optimization of aerogel synthesis is an essential step for preparing the starting recipe for aerogel-modified EP. Firstly, t**he concentration of oxalic acid** was studied while fixing all steps and variables in these steps. In other words, only the concentration of the acid catalyst was varied, and the flowchart of the aerogel synthesis in Figure 13 was followed. In order to

determine the determine necessary concentration of oxalic acid, the aerogels were prepared by keeping the molar ratio of TEOS:EtOH:H_2O constant at 1:5:7 and the concentration of the ammonia base catalyst was fixed at 1 M. The acid catalyst was varied systematically from 0.001 M to 0.02 M increased by 0.001.

After the determining of the concentration of the oxalic acid catalyst, **the amount of base catalyst** was changed systematically while fixing all variables and following the flowchart of the aerogel synthesis. The amount of base catalyst was examined by keeping the molar ratio of TEOS:EtOH:H_2O constant at 1:5:7 with the oxalic acid catalyst concentration was fixed at 0.02 M (as a result of oxalic acid catalyst concentration optimization experiment). The ammonia base catalyst was fixed at 1 M, and the amount was changed from 1 ml to 10 ml by 1 ml increment. The success of the aerogel synthesis means that the synthesis is optimized. When the synthesis optimization was completed, the second part was initiated.

3.3.2. Part 2: Aerogel-Modified Expanded Perlite (AEP) Synthesis

25 ml TEOS, 125 ml EtOH and were poured into the 500 ml beaker and were mixed. In this case, **the amount of perlite** needs to be used in the aerogel-modified expanded perlite synthesis had to be decided. Therefore, the amount of

perlite was studied by varying from 10 gr to 45 gr increased by 5 gr. Expanded perlite aggregate was added to the beaker and was stirred by hand. 5 ml of the oxalic acid catalyst with the optimized concentration was added to the solution with the glass pipette and the beaker was covered. The beaker was stirred by hand for 30 min, then was placed on the flat surface. After 24 hours, an ammonia base catalyst with the optimized amount was added to the solution dropwise while the beaker was stirring. The solution was transferred to the molds with piston and the mold caps were made airtight as demonstrated in Figure 15 (a). After gelling occurred, samples were ejected from the molds with the help of pistons (Figure 15 (b)). Then, the gels were waited in EtOH for 6 hours and then in n-hexane/TMCS (5:1 V/V) for 24 hours for aging. Gels were exposed to 60 °C for 4 hours, 80 °C for 2 hours, 120 °C for 2 hours, and 200 °C for an hour heat treatment in Nüve muffle furnace. The photograph of the samples in the furnace is shown in Figure 14. The flowchart of the aerogel-modified expanded perlite synthesis is given in Figure 13 (right).

Figure 14 The photograph of the sample in Nüve muffle furnace before the heat treatment

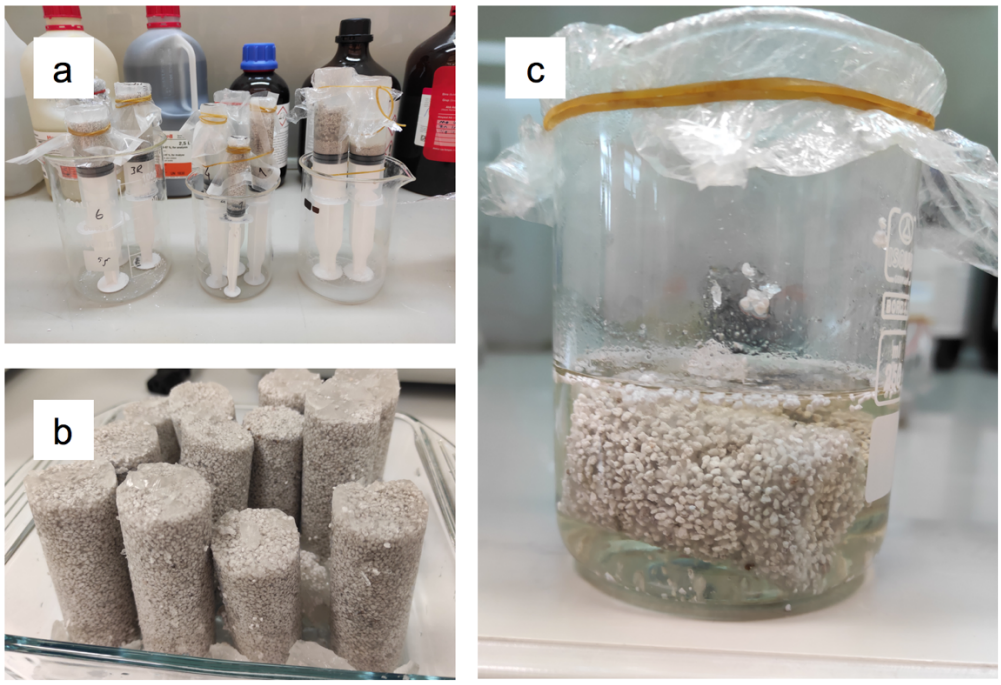

Figure 15 (a) Photographs of samples in airtight molds, (b) samples ejected from the molds, and (c) the sample in EtOH

Characterization tests followed the synthesis of aerogel-modified expanded perlite. After ensuring by characterization tests that aerogel-modified expanded perlite was obtained, the board production step was started.

3.3.3. Characterization Tests for Aerogel-Modified Expanded Perlite (AEP)

3.3.3.1. Sintering of Aerogel-Modified Expanded Perlite

The high temperatures are reaching 900 °C cause shrinkage and sintering of perlite. The shrinkage leads to deformation on particles and increasing thermal conductivity. Therefore, performing the drying process at low temperatures is significant for both gel and perlite structures. On the other hand, after the synthesis is completed, aerogels are endurable at high temperatures. The aerogel network inside and the surface of perlite protects the structure from high temperatures such as sintering. The sintering behavior of AEP was presented by high-temperature heat treatment in Nüve muffle furnace. The annealing process consists of 5 hours of heating up to 550 °C, 5 hours of heating from 550 to 850 °C, 4 hours of constant heating on 850 °C was applied to EPA, synthesized aerogel and AEP. Additionally, heat treatment of 1100 °C for 4 hours was applied to the particles.

3.3.3.2. Microstructural analysis of Aerogel-Modified Expanded Perlite

FEI Scanning Electron Microscopy (SEM) device in National Nanotechnology Research Center (UNAM) was used to analyze the surface of aerogel-modified expanded perlite particles before and after modifications and treatments. The microstructure of an AEP includes visual demonstrations of shells of perlite pores. Expanded perlite aggregate and aerogel-modified expanded perlite particles were placed on the pins. These particles were coated in a sputtering device in order to prevent the scattering of perlite particles under electron

bombardment inside SEM. The coating operation was carried by the gold/ palladium (Au/Pd) sputter coater in National Nanotechnology Research Center (UNAM).

3.3.3.3. Loose Bulk Density and Specific Gravity of Aerogel-Modified Expanded Perlite

The loose bulk density of aggregates was measured according to TS EN 1097-3 standard. *The loose bulk density* is the uncompressed dry aggregate loose density in a given measuring container. For measurement, three sets of EPA particles were dried at 110±5 °C in Nüve dry air sterilizer oven until no weight change is observed. The empty container was weighted (m_1) and filled with EPA until they overflow from the container. The top surface of the container was leveled by rolling a rod on it. The container was weighed again and noted as m_2 with 0.1% precision. These steps were repeated for three sets of EPA. The loose bulk densities of aggregates were calculated according to the equation below.

$$\rho b = (m_2 - m_1) / V$$

where;

ρb : Loose bulk density of aggregate (g/cm^3)

m_2 : Container and sample weights (kg)

m_1 : Empty container weight (kg)

V : Container volume (L)

Specific gravity is the fraction of the mass of the sample without empty spaces to the weight of a unit volume of given reference material. The measurement was carried by Le Chatelier flask for aggregates according to TS 2511 standard. Samples were dried at 110±5 °C in Nüve dry air sterilizer oven until no weight change was observed. The neck of the flask was graduated from 0 to 0.1 ml subdivisions above and below of the oval bulb on the neck. The kerosene was poured between 0 to 1 ml point on the neck, and the stopper was inserted. The aggregates were ground in the ceramic mortar and sift through the sieve. The equipment for the specific gravity measurement is given in **Figure 16** (a). Then, the ground sample was poured slowly and carefully into the flask with the help of a glass funnel. After the material was wholly transferred to the flask, the stopper was inserted, and the flask is rotated around its axis for allowing the air mixed with the sample powders to escape. This process was repeated until it was ensured that the air bubbles were removed entirely. The volume was read, and the specific gravity was calculated by the dry weight ratio by final and initial volume differences, as demonstrated in the following equation.

$$\mathbf{SG = W / V_C}$$

where;

SG : Specific gravity (g/cm^3)

W : Weight (g)

V_C : Volume change, the volume difference of final and initial volumes (cm^3)

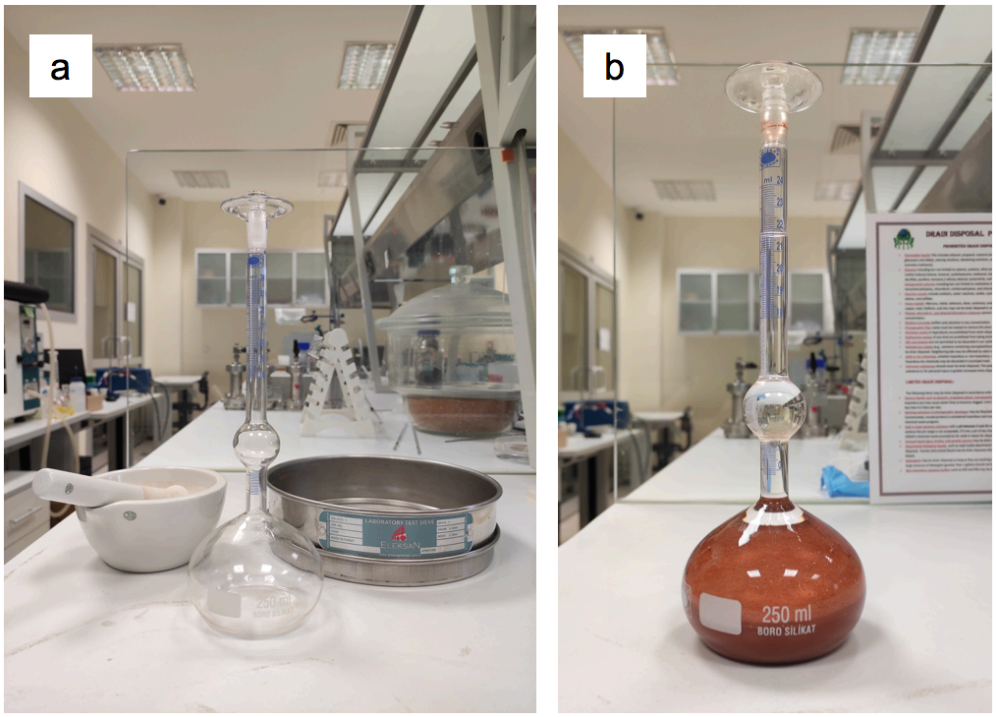

Figure 16 (a) The equipment for determining the specific gravity; the ceramic mortar, Le Chatelier flask, and the sieve. (b) The Le Chatelier flask containing the powdered sample and kerosene.

3.3.4. Part 3: Aerogel-Modified Expanded Perlite/Clay (AEP/C) Board Production

This part of the study was concerned with preparing an AEP composite made of clay-based aerogel-modified expanded perlite and testing the physical and mechanical performances of the composite boards, as illustrated in Figure 10. Clay was employed as a binder material in this study. The aerogel-modified expanded perlite was used as filler material. The aggregates were synthesized and used with clay to produce an AEP/C composite board. The illustration of an AEP/C composite is represented in Figure 17.

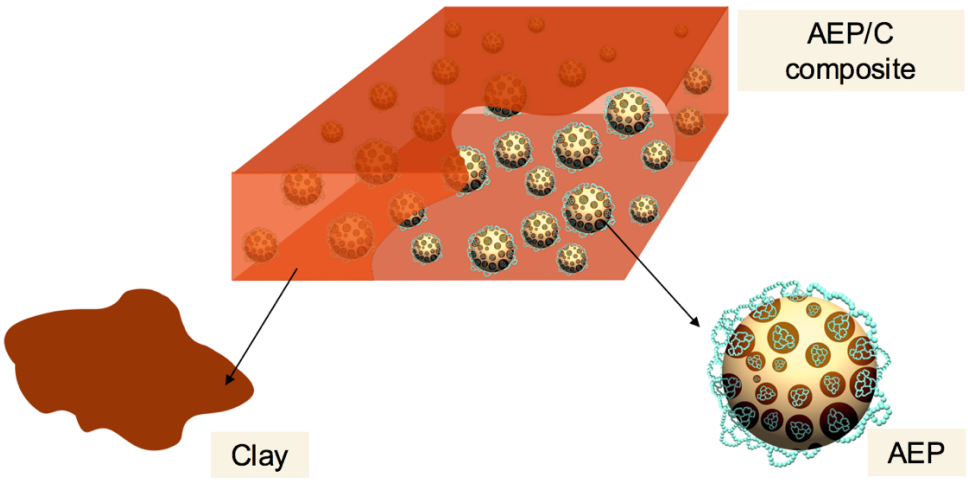

Figure 17 The representation of AEP/Clay composite board

A previous study offers the optimum process and composition of EP/clay-based exterior wall thermal insulation board as 50% clay and 50% EPA by weight. The ratio corresponds to 5% clay and 95% EPA by volume (Yilmazer, 2018). In parallel with this study, equal weights of EPA and clay were used for the EP/C control sample board. Similarly, equal weights of AEP and clay were used for the AEP/C composite boards. Clay and perlite were dried at 105 °C in Nüve dry air sterilizer oven until no weight changes were observed. Clay was ground and brought into powder form. The powdered clay was then sieved. 80 gr each of clay and AEP were weighted with precision balance and were filled into a soft container. It was shaken by hand until the dry mixture seems homogeneous. The dry mixture was poured into a vessel, as shown in Figure 18 (a). DH_2O was added dropwise, and the mixture was stirred constantly. The addition of DH_2O was continued until the viscosity of AEP and clay was sustained (Figure 18 (b)).

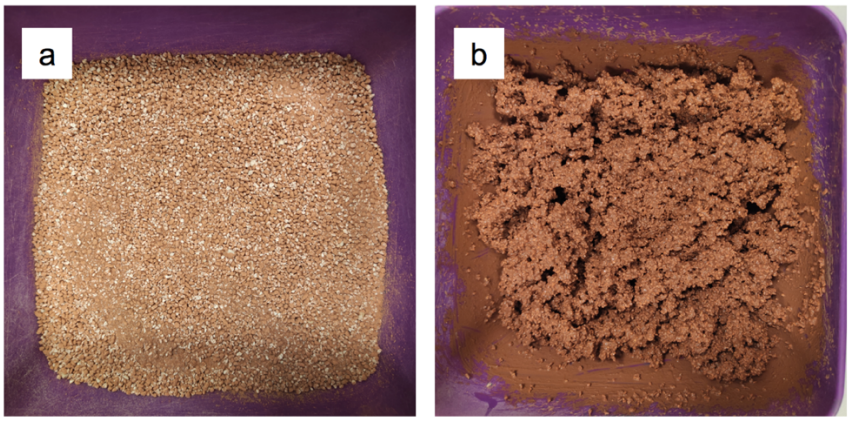

Figure 18 (a) Dry clay and AEP mixture and (b) in a mortar form after DH_2O was added

The mixture was discharged in the wooden mold with the help of a spoon and pressed. The mold was placed on the vibrator in order to settle particles, make them close to each other and increase the bonding. After 5 minutes of vibration, the mold was covered with a film layer to insulate from the air and keep the natural humidity, and allowed to wait 24 hours. It was held on uncovered waiting for 24 hours. It was put into the drying oven immediately afterward to dry for 48 hours. The board was removed from the mold, and heat treatment was carried. This annealing process consists of 5 hours of heating up to 550 °C, 5 hours of heating from 550 to 850 °C, 4 hours of constant heating on 850 °C in Nüve muffle furnace. Then, the sample was left to cooling until reaching room temperature. After reaching room temperature, boards were taken out from the furnace (Figure 19). The preparation of the AEP/C board is summarized in illustration at Figure 20.

Figure 19 The photograph of boards after the process was completed

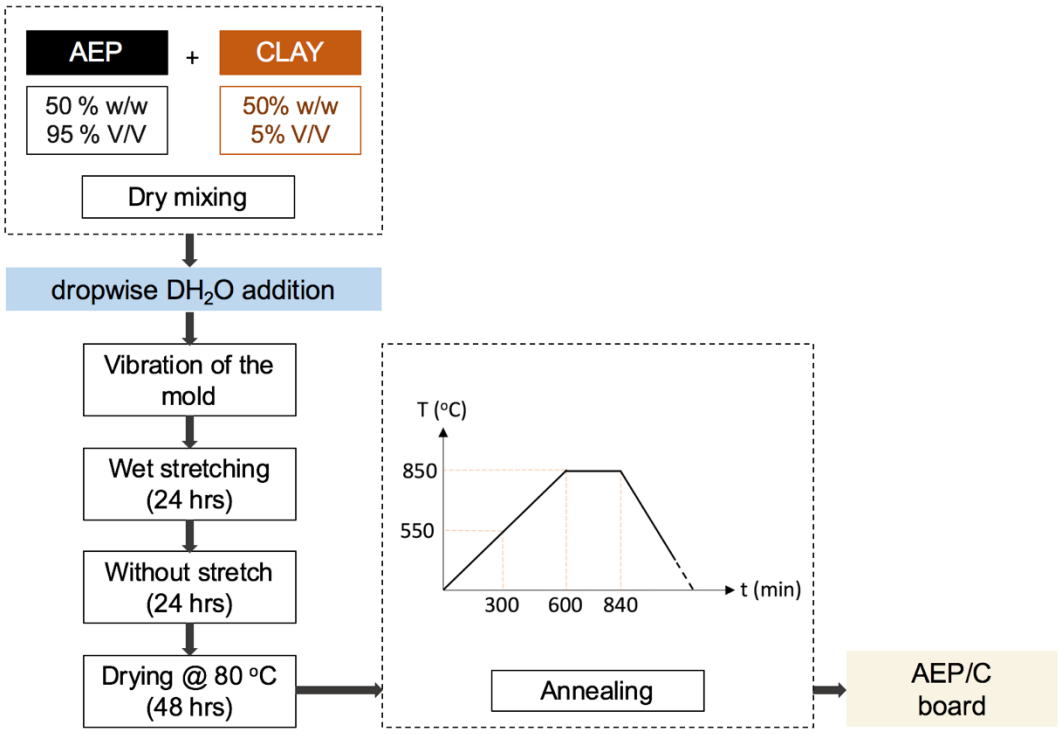

Figure 20 The schematic of preparation of aerogel-modified expanded perlite/clay composite board

3.3.5. Characterization Tests for Aerogel-Modified Expanded Perlite/Clay Board

Aerogel-modified expanded perlite/clay boards were subjected to microstructural analysis, unit volume mass and specific gravity calculations, water absorption test, and three-point flexural test (bending strength test).

3.3.5.1. Microstructural Analysis of Aerogel-Modified Expanded Perlite/Clay Board

FEI Scanning electron microscopy (SEM) device in National Nanotechnology Research Center (UNAM) was used to analyze the morphology of the internal surface of AEP/C boards. The boards were sliced carefully, and cross-section specimens were placed on the pins. These samples were coated in the sputtering device to prevent the damage and charging of specimens under electron bombardment and high vacuum inside SEM. The coating operation was carried by the gold/ palladium (Au/Pd) sputter coater in National Nanotechnology Research Center (UNAM). The voltage is generally chosen as 5 kV in SEM in order to examine the structures formed on the surface with precision.

3.3.5.2. Unit Volume Mass and Specific Gravity of Aerogel-Modified Expanded Perlite/Clay Board

The weight of sample boards was determined according to TS 3649 standard. The dimensions of boards were measured with 0.1 mm precision. The volume of the boards with a void area was found. Unit volume mass (UVM) of boards was calculated according to the equation below.

UVM = m / V and **V = l*b*d**

where;

UVM : Unit volume mass of a board (g/cm^3)

m : Board weight (g)

V : Board volume (cm^3)

l : Board length (cm)

b : Board width (cm)

d : Board thickness (cm)

The specific gravities of boards were calculated by the measurements carried by the Le Chatelier flask for blocks according to TS 2511 standard. Boards were dried at 110±5 °C in Nüve dry air sterilizer oven until no weight change was observed. Then, the boards were ground in the ceramic mortar and sift through the sieve. The consecutive steps were the same as the specific gravity test for aggregates given above. The photograph of the Le Chatelier flask containing the powdered board sample and kerosene is demonstrated in Figure 16.

3.3.5.3. Water Absorption of Aerogel-Modified Expanded Perlite/Clay Board

The water absorption tests of boards prepared by EPA (control sample boards) and AEP (AEP/C boards) were conducted according to TS EN ISO 29767

standard. The boards were dried at 110±5 °C in Nüve dry air sterilizer oven until constant weights were observed, and weights were noted (W_D). The boards were allowed to remain submerged in water for 48 hours. They were removed from the water and weighed (W_W). The following formula calculated the volume of voids.

$$\mathbf{V_V = (SP - \rho / SP) * V}$$

where the density was calculated by

$$\mathbf{\rho = W_D / V}$$

and where;

V_V : Volume of voids (cm^3)

SG : Specific gravity

ρ : Density (g/cm^3)

W_D : Initial weight of dry sample (g)

W_W : Wet weight (g)

V : Total volume (cm^3)

Porosity was calculated to the equation below.

$$\mathbf{n = V_V / V}$$

where the porosity is denoted by n.

Finally, the boards' water absorption (WA) was evaluated with the ratio of absorbed water and the dry weight. Hence, the water absorption rates of boards were calculated by the following formula.

$$\mathbf{WA = ((W_W - W_D) / W_D) * \%}$$

where;

WA : Water absorption

W_W : Wet weight (g)

W_D : Initial weight of dry sample (g)

3.3.5.4. Bending Strength of Aerogel-Modified Expanded Perlite/Clay Board

The bending strength is the ability to resist deformation under load. The strength of boards was determined according to TS EN 12089 standard. The measurement was carried by bending-stress measuring equipment, as shown in Figure 21(c). The mechanical strength of the boards was determined with the three-point flexural test. The board was placed on two parallel supporting points in this test, as shown in the schematic and the photo in Figure 21 (a), (c). The loading force was implemented in the middle of the board. The force applies uniformly in this configuration. When the concentrated load is performed at the center, the board starts to bend concave downwards, as represented in Figure

21 (b). he board was failed at the maximum load. The maximum force applied to the board was read on the screen and noted. The flexural strength of the board was calculated in the formula below.

$$\sigma = 3LF / (2bd^2)$$

where;

σ : Bending strength, flexural strength

L : Distance between supports (mm)

F : Total force applied to the board (N)

b : Board width (mm)

d : Board thickness (mm)

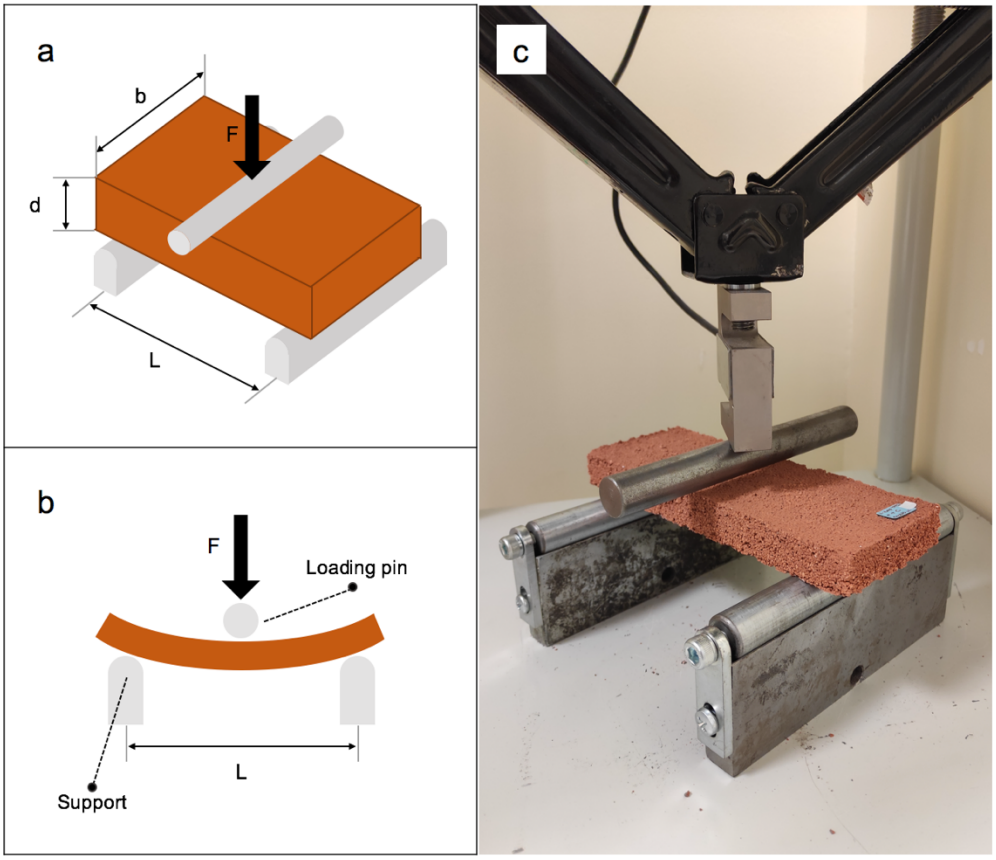

Figure 21 (a) The axonometric representation and (b) side view of a schematic of flexural strength, and (c) the photograph of bending test machine and the board before testing (Illustrations are drawn by the author)

CHAPTER IV

RESULTS AND DISCUSSION

This research hypothesized that there is a contribution to the mechanical strength of clay-based aerogel-modified expanded perlite board. In order to understand this, the aerogel synthesis process was optimized, and then the process was applied to aerogel modification on EPA. The amount of EPA for this process was optimized. Synthesized aerogel-modified expanded perlite particles were used for aerogel-modified expanded perlite/clay boards. The physical and mechanical characterization and tests were carried. This chapter will focus on significant findings and results and discussing their relations and contradictions with literature.

4.1. Part 1: Aerogel Synthesis

The optimization of the aerogel synthesis provided the starting procedure for the consecutive parts. The concentration of oxalic acid and the amount of base catalyst needed for this acid concentration were studied.

The acid catalyst concentration was studied by systematically varying the molarity from 0.001 to 0.02 M, increased by 0.001, and fixing the acid catalyst amount at 10 ml. The experiments for 0.001 to 0.009 M showed no gelation despite long waiting times for days. On the other hand, it was observed that gelation started in experiments prepared with 0.01 M; however, gelation required long waiting times. In the experiments prepared with 0.02 M, the gelation took place in a day, which is the optimum time and the other test parameters.

The amount of base catalyst was examined by varying the amount from 1 to 10 ml increased by 1 ml while the concentration was fixed at 1 M. There was no gelling observed after a day on the experiments prepared with 1 to 4 ml base catalyst. The gelling was observed in the experiments done with a 4 ml base catalyst after three days. While the amount was increasing, the gelling time was decreased. On the other hand, the experiments prepared with a 5 ml base catalyst showed gelling for a day. The addition of 6 to 10 ml base catalyst caused

rapid gelation, and cracks were observed on the surface of gels prepared with 8 to 10 ml base catalyst.

The increase in the base catalyst amount increases condensation reactions leading to the lowering of gelation time. The solution catalyzed only by the acid catalyst in a lower base catalyst (1-4 ml) had a longer gelation time. This process leads to a decrease in the reaction rate and hinders little crosslinking in the gel network. On the other hand, this sudden condensation will cause many fractures on the surface and volume shrinkage in the drying process (Rao & Bhagat, 2004). Based on the results, it was decided to continue the experiments using a 5 ml base catalyst with a concentration of 1 M.

The experiments resulted without gelation are explained by the insufficiency of the catalysts in terms of amount or concentration. On the other hand, the high amount or concentration of catalysts caused rapid gelation and caused changes in the structure of the aerogels (Rao & Bhagat, 2004). This acid-base catalyst balance is significant in hydrolysis and condensation reaction rates (Dorcheh & Abbasi, 2008).

According to Dorcheh & Abbasi (2008), The duration of chemical reaction proceeds is related to the relative rate of reaction. While the oxalic acid catalyst

is added to the solution, randomly branched chains start to constitute in the sol. Gelation duration is longer if the pH of the sol is low. Therefore, the ammonia base catalyst was incorporated in the sol to accelerate the reaction, thus reduce the gelation time while increasing the pH of the solution. As the base catalyst was added to the mixture, the condensation reaction kinetics gets faster than hydrolysis reaction kinetics. This leads to uniform network formation. Figure 22 depicts the relationship between the relative rate of reaction for hydrolysis and condensation.

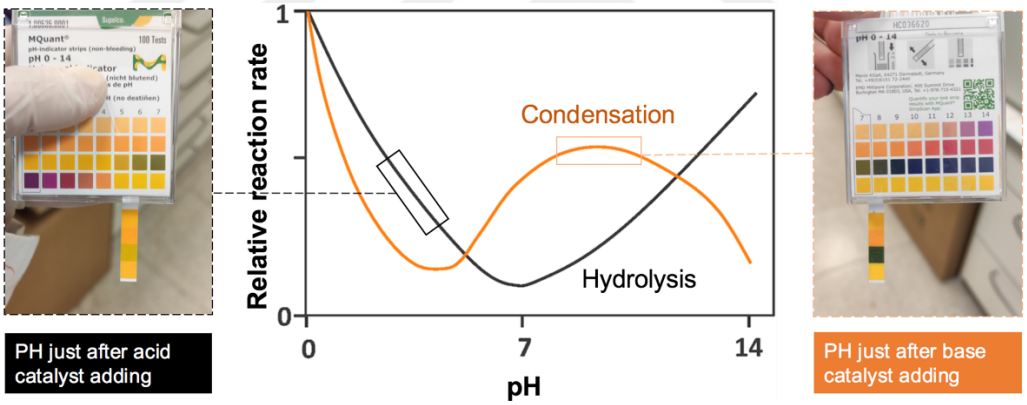

Figure 22 pH analysis of solutions just after the adding of oxalic acid (left) and ammonia (right), and the relationship between the relative hydrolysis and condensation and the pH of the solution (middle, drawn by the author based on the graph in the study of Dorcheh & Abbasi (2008))

The litmus paper was used to measure the pH of the solutions in experiments, as shown in Figure 22. Gelation was observed if the pH was in the acidic pH region

(pH from 0 to 6) after adding the acid catalyst and in the basic pH region (pH from 8 to 14) after the base catalyst was added. Depending on the acid catalyst concentration, either no or very little gelation was observed if the pH was outside this acid range after adding the acid catalyst. After adding the acid catalyst, the base catalyst was added to the solution with a pH value in the acidic region. If the amount of base catalyst was insufficient to pass into the basic pH range, either little or no gelling was observed after very extended gelation times. In other words, the pH values in the experiments that resulted without gelation were not in the specified pH range of hydrolysis and condensation shown in the graph in Figure 22. Therefore, it was concluded that measuring the pH of the solutions after adding catalysts is essential for the aerogel synthesis via the sol-gel method.

4.2. Part 2: Aerogel-Modified Expanded Perlite (AEP) Synthesis

How much of the solution used will penetrate the pores of the perlite and the amount of solution required to cover the surfaces of the EPA particles are significant while preparing the AEP. Therefore, the amount of EPA required for the system needs to be examined. EPA amount for AEP synthesis was investigated by changing EPA amount from 10 to 45 gr by 5 gr increment. The use of from 10 gr to 35 gr perlite leaded excessive chemicals in the medium. On the other hand, 45 gr perlite was excess for the solution and caused chemical

inadequacy for the reactions. The insufficient chemicals caused the aerogel formation inside the pores of perlite particles; however, the lack of aerogel required for the adhesion was observed of the perlite particles. The optimum amount of EPA for AEP synthesis was determined as 40 g.

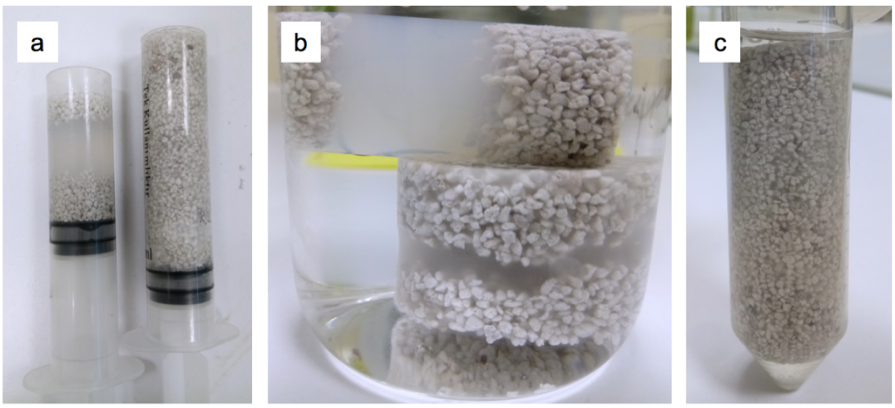

Figure 23 Photos of (a) the excess chemicals between aerogel-perlite blocks (left) and insufficient chemicals that caused nonadherent perlite particles (right) in the molds; (b) the use of 15 gr (up) and 25 gr perlite (bottom) and excess aerogel between aerogel-perlite blocks; and (c) the use of 40 gr perlite that is the optimum amount for the synthesis

4.2.1. Sintering Test and Microstructural Analysis of Aerogel-Modified Expanded Perlite

The annealing process for the boards consisting of 5 hours of heating up to 550 °C, 5 hours of heating from 550 to 850 °C, 4 hours of constant heating on 850 °C

was applied to aerogels, EPA, and AEP particles. There was no structural or color change was observed on particles after the heat treatment. Therefore, samples were subjected to additional heat treatment at 1100 °C for 4 hours. The EPA particles were sintered after the high-temperature treatment, and their color shifted from white to pinkish, and they significantly lost their volume. On the other hand, the treatment did not affect the AEP particles and the aerogels in terms of color and structural changes. This is an impression that the EPA particles are surrounded by aerogel, and aerogel modification is an effective way to prevent the sintering and shrinkage of EPA. This was a manifestation that EPA can be resistant in fire cases with high temperatures. The photographs of the EPA, AEP and the aerogel in Figure 24 present the physical changes of EPA and the durability of AEP and aerogels after the treatment.

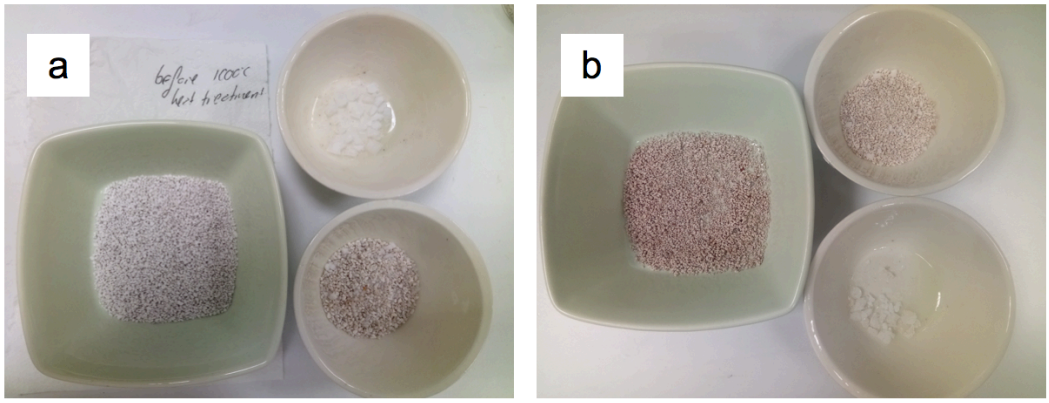

Figure 24 (a) The photo of a EPA without treatment (in the square-shaped mortar), aerogel (up, rounded shape mortar), AEP (down, rounded shape mortar) before 1000 °C heat treatment for 4 hours. The photo of (b) the EPA (in the

square-shaped mortar), aerogel (down, rounded shape mortar), AEP (up, rounded shape mortar) after the high-temperature treatment.

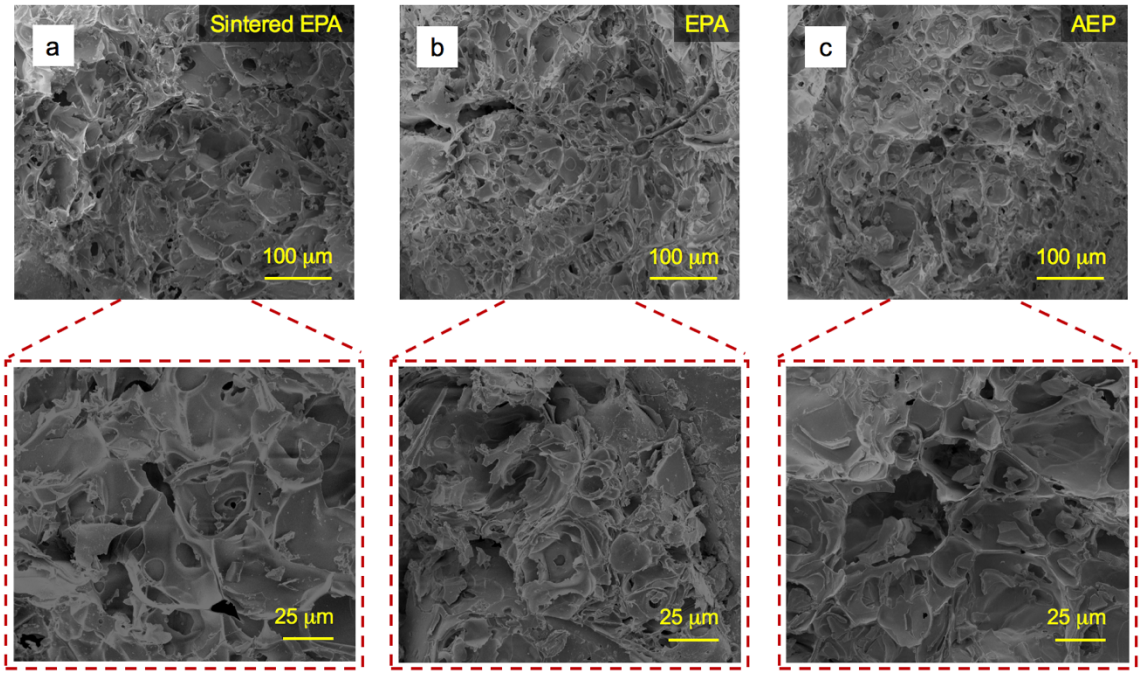

Figure 25 SEM images of the surface morphology of (a) EPA after sintering, (b) EPA, and (c) AEP

The surface structures of the EPA, sintered EPA, and AEP were examined by scanning electron microscopy. The surface of EPA consisted of open and closed pores, which seem divided by wrinkled shells (Figure 25 (b)). Examination of the SEM images pointed out that there were crystal-like porous structures with no dominant geometry. SEM images were similar to SEM images of the previous study of Celik, Kilic, and Cakal (2013). The sintering of EPA caused flattened

surface geometries and large pore borders (Figure 25 (a)). Actually, these borders consisted of more than one pore of EPA without heat treatment. The high-temperature annealing yielded the intertwine of surface microstructures during shrinkage. On the other hand, aerogel modification of EPA was inclined to fill the pores and covers the surface (Figure 25 (c)). As shown in the zoom image of AEP in the Figure 25 (c), shells of pores and the aerogel coverage over pores were seen.

4.2.2. Density and Specific Gravity of Aerogel-Modified Expanded Perlite

Three expanded perlite aggregate and aerogel-modified expanded perlite samples were used for the loose bulk density calculation in accordance with TS EN 1097-3. The mean values of samples and standard errors were calculated via Excel. The specific gravities of EPA and AEP were calculated by using Le Chatelier flask in accordance with TS 2511 standard. According to the calculations, EPA has loose bulk density 0.21 g/cm^3 and a specific gravity of 1.8±0.01 g/cm^3 at ambient temperature. AEP has loose bulk density 0.26±0.01 g/cm^3 and a specific gravity of 1.93±0.09 g/cm^3. The values were summarized in Table 3. The loose bulk densities of EPA and AEP were within the range of loose bulk density of expanded perlite given as 0.032-0.4 g/cm^3 by Perlite Institute; however, specific gravities were below the range of 2.2-2.4 (www.perlite.org).

Loose bulk density is calculated with a volume of the container filled with the particles. Therefore, this volume consists of both volumes of particles and volume of spaces between the particles. This phenomenon is called **The Kepler conjecture**. This theory represents the highest packing density of spheres in the three dimensional space (Yılmazer, 2018). Aerogel modification did not change the spherical form of the particles. Therefore, the loose bulk densities of both control particles and aerogel-modified aggregates behaved by this theory. The slight increase in aerogel-modified particles depended on the contribution of aerogel, which is inside the pores and the surface of the particles, to the density.

On the other hand, specific gravity gives the density of particles without the volume of space, because of the reduction in the volume occupied by the powdered particles. Therefore; the specific gravities of particles were higher than loose bulk densities. Approximately 0.1 g/cm^3 difference between the specific gravities of EPA and AEP particles arose from aerogel modification. The difference in specific gravity between the two porous structures (such as EPA and AEP) gives an idea about their porosity. If the specific gravity of a structure is higher than the other, it means that there will be more solid weights in the same filled volume. Therefore, it can be said that this structure has less porosity. Aerogel modification caused the filling of the pores of perlite. However, aerogel itself has a porous structure like EPA. Therefore; there was a slight increase in specific gravity although the aerogel filling inside pores.

Table 3 Loose bulk density and specific gravity values of EPA control sample and AEP sample

EPA (control sample)	
Loose bulk density (g/cm^3)	Specific gravity (g/cm^3)
0.21	1.8 ± 0.01
AEP	
Loose bulk density (g/cm^3)	Specific gravity (g/cm^3)
0.26 ± 0.01	1.93 ± 0.09

4.3. Part 3: Aerogel-Modified Expanded Perlite/Clay (AEP/C) Board Production

A microstructural analysis, density and specific gravity calculations, water absorption test and three-point flexural test results of aerogel-modified expanded perlite/clay boards were given below.

4.3.1. Microstructural Analysis of Aerogel-Modified Expanded Perlite/Clay Board

The internal surface of the boards was revealed by scanning electron microscopy (SEM). As can be seen in Figure 26 (a) and its close-up image right, the EP/C

control sample has perlite particles with a three-dimensional cellular structure composed of both open and closed cells. Many of the closed cells were broken during slicing for SEM preparation. Clay has a bulky structure and covers both the outer surface of perlite and inside of some of open pores of perlite.

The microstructure of an AEP/C board consists of aerogel, clay, open and close pore shells of perlite as shown in Figure 26 (b). SEM images demonstrated that aerogel structures filled the perlite pores and covered the surfaces after the aerogel modification on the aggregates. This image was very similar with the study of Jia et al. (2018). The surface of the aerogel in our study resembled the study of Peng & Yang (2013). In this study, the existence of the aerogel inside the expanded perlite was shown with the SEM image of the aerogel/expanded perlite composite. When these particles were bound with clay, clay matrix covered the outer shell surfaces of the particles and kept them together. This means that in cases where the aerogel-modified perlite particles are in the system, the pores through which the clay penetrates in control board samples are now filled with aerogel. Therefore, clay was observed only on the shell surfaces of aerogel-modified expanded perlite particles in SEM images of the interior surfaces of AEP/C board.

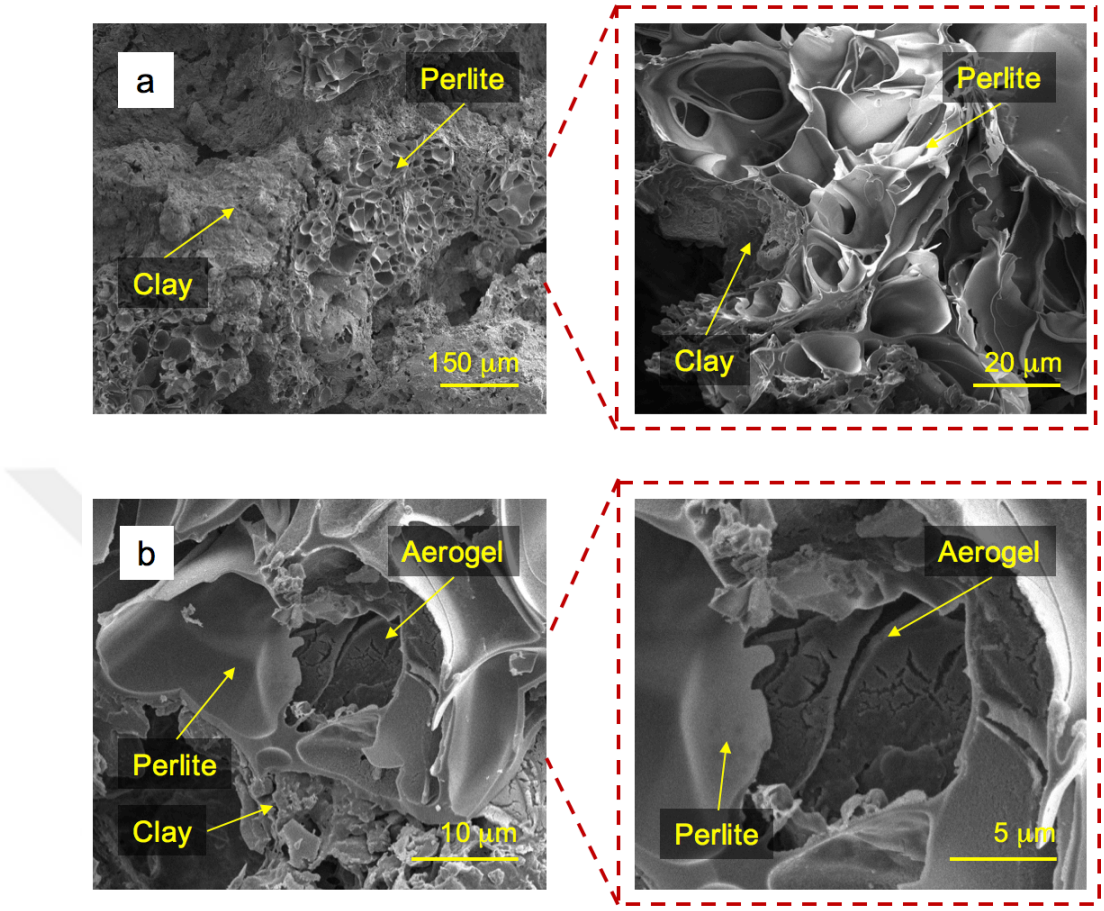

Figure 26 SEM images of internal surfaces of (a) EP/C (control sample board) and (b) AEP/clay composite boards. Close-up SEM images are shown right side of the images

4.2.2. Unit Volume Mass and Specific Gravity of Aerogel-Modified Expanded Perlite/Clay Board

Unit volume mass and specific gravity calculations were carried according to the equation given in the chapter of *Experimental Study*. The unit volume masses of

five AEP/C and EP/C control boards were calculated. The mean of unit volume mass of samples and standard errors were calculated by Excel. The unit volume mass of EP/C control board samples was found as 0.46±0.02 g/cm^3. The unit volume mass of AEP/C boards was 0.55±0.01 g/cm^3. Unit volume mass means mass per unit volume of a sample board. The volume includes both solid and void areas of the board. Clay occupies the spaces between the packed particles, which is mentioned in *Section 4.2.2* as The Kepler conjecture. However, clay is used in both the EP/C control board and AEP/C board preparation; hence, the space volume between particles is filled with clay in both cases. On the other hand, aerogel covered the surfaces of perlite particles and filled some of the open pores of the particles. In this case, clay did not penetrate these pores that filled with aerogel. Additionally, aerogel substituted some of the pores of particles that clay did not occupied in any case. As a result, the aerogel modification caused a slight increase in the unit volume mass. The UVM calculations for all boards and mean values were demonstrated in Table 4.

The specific gravity represents the density of boards without the volume of space. It was calculated with the Le Chatelier flask. Five AEP/C board samples and five EP/C board control samples were used for the testing. The mean values of samples and standard errors were calculated via Excel. According to the calculations, the mean of specific gravity of EP/C samples was 2.33±0.02 g/cm^3 and AEP/C was 2.36±0.01 g/cm^3 as given in Table 4. Aerogel modification of

particles slightly affected the specific gravity of the boards as compared to aerogel-free boards.

These results were higher than the UVM value of 0.27 g/cm^3 of expanded perlite/clay-based board in the previous study of Yılmazer (2018). Similarly, the specific gravity of EP/C was higher than the specific gravity of 2.07 g/cm^3 in the previous study. The same clay was used in both studies. This difference could be depended on the type of EPA used in the board production. The source region of EPA determines the properties of particles.

Considering the unit volume mass of the boards in our study, the slight change on UVM value was advantageous in two aspects. Firstly; it was possible to estimate that the aerogel modification of perlite does not cause a noticeable additional weight of AEP/C boards. Secondly, keeping the UVM ratio low is significant to the thermal resistance of porous materials, even the sound absorption coefficient (Yılmazer, 2018). The modification of the aerogel slightly altered the UVM value and indicated that it would not cause a remarkable effect on the thermal conductivity via density-related variables. On the other hand, thermal conductivity of aerogel is lower than air, as aforementioned above sections. Therefore, it can be estimated that the AEP/C composite may have approximately equal or lower thermal conductivity than the EP/C control board.

Therefore, to verify this inference, the thermal conductivity measurement of the produced boards is needed.

Table 4 Unit volume mass and specific gravity values of EP/C control sample boards and AEP/C sample boards

Unit volume mass and specific gravity						
EP/C (Control sample)						
	Sample 1	Sample 2	Sample 3	Sample 4	Sample 5	Mean
Unit volume mass (g/cm^3)	0.49	0.46	0.43	0.51	0.43	0.46 ± 0.02
Specific gravity (g/cm^3)	2.35	2.32	2.29	2.37	2.30	2.33 ± 0.02
AEP/C						
	Sample 1	Sample 2	Sample 3	Sample 4	Sample 5	Mean
Unit volume mass (g/cm^3)	0.54	0,56	0.58	0.54	0.54	0.55 ± 0.01
Specific gravity (g/cm^3)	2.32	2.37	2.39	2.35	2.36	2.36 ± 0.01

4.2.3. Water Absorption of Aerogel-Modified Expanded Perlite/Clay Board

The dry weights of boards after dried at 110±5 °C in drying oven until constant weights (W_D) and wet weights of boards after 48 hours (W_W) were obtained. The volume of voids, porosity and water absorption capacity of boards were computed according to equations in *Section 3.3.5.3*. Mean values and errors were calculated. According to results; *volume of voids* of the EP/C board is 40.51, and 36.23 ± 1.05 for the AEP/C board. Aerogel modification caused

tenuously filling some of the open pores with a solid skeleton of the aerogel. Therefore; the volume of voids lightly decreased with the aerogel modification. On the other hand; the *porosity* is the percentage expression of the proportion of the total void volume and whole volume. Results showed that the porosity of EP/C was 0.78% and this is 0.77% for AEP/C. Although there is very little difference between the void volume results of EP/C and AEP/C boards, it appeared that composite boards still retained their porosity when the void to total volume ratio is expressed as a percentage. In other words, aerogel-modified perlite still retained its highly porous structure depending on the intrinsic porous structure of aerogel. Therefore, it can be interpreted as the aerogel modification provided the continuity of the total porosity.

The water absorption of EP/C control board was 86.28%, the water absorption of the AEP/C board slightly decreased to 83.91 ± 0.49%. When the water absorption percentages of the EP/C and AEP/C boards were compared, a slight reduction in the water absorbance of the boards was provided by aerogel modification. It is known that moisture retention is a problem in plates made of perlite and studies have been carried out to water retarding quality of perlite-based plates (Yılmazer, 1998). Therefore, observing that water absorbance did not increase in the aerogel-modified plates is promising for future researches.

4.2.4. Bending Strength of Aerogel-Modified Expanded Perlite/Clay Board

The three-point flexural test revealed the bending strength of boards. In the bending test, when the force is applied, concave side of the board is subjected to tension, and the convex side is exposed to maximum stress. Failure is observed when the strain or elongation exceeds the material's limits. The force on the screen at the failure point is recorded as F value, and the flexural strength was calculated.

Table 5 The bending strengths and mean values of EP/C control sample and AEP/C sample boards

Bending strength (N/mm^2)					
EP/C control boards					
Sample 1	Sample 2	Sample 3	Sample 4	Sample 5	Mean
0,63	0,69	0,68	0,72	0,76	0.7 ± 0.02
AEP/C boards					
Sample 1	Sample 2	Sample 3	Sample 4	Sample 5	Mean
0.74	0.66	0.62	0.77	0.84	0.73 ± 0.04

The bending strengths of EP/C control boards were from 0.63 to 0.76 N/mm^2 and the mean value of strengths was calculated as 0.7 ± 0.02 N/mm^2. On the other hand, the flexural strengths of AEP/C boards were from 0,62 to 0.84 N/mm^2 and

the mean of their bending strengths was 0.73 ± 0.04 N/mm^2. Although some of the bending strength of AEP/C boards slightly higher than EP/C control sample boards; the mean value of bending strength of AEP/C boards was equal to EP/C boards, approximately (Table 5).

The unit volume mass (UVM) and bending strength graphs in Figure 27 represents the correlation between UVM and the bending strength of the boards. In other words, the graph shows either the aerogel modification affects the bending strength of the boards or not. The unit volume mass and bending strength graph for EP/C control boards demonstrated that as the UVM of the plates increases, the flexural strength also increased with a general trend in parallel with the previous study (Yılmazer & Baytekin, 2017). On the other hand, two control samples with UVM value of 0.43 g/cm^3 had 0.63 and 0.68 N/mm^2 bending strength values. The flexural strength changed without the density change. This situation can be explained by the defects in the boards. Some of the board samples had undesirable cracks on the surfaces because of the experimental conditions. These cracks on the board surfaces may cause the board to break under a lower force than it should be, due to the force applied during the bending strength test. Another reason can be related to the squeezing pressure applied by hand after the clay, perlite and DH_2O mixture were poured into the wooden molds. As it is known, the extra pressure applied during the board preparation process has an effect on increasing the strength of the boards. For this reason, it was observed that the flexural strength value that the board

density should provide is lower. However, it should be taken into account that the density changes between the boards were very small and that caused also slight changes in the bending strengths.

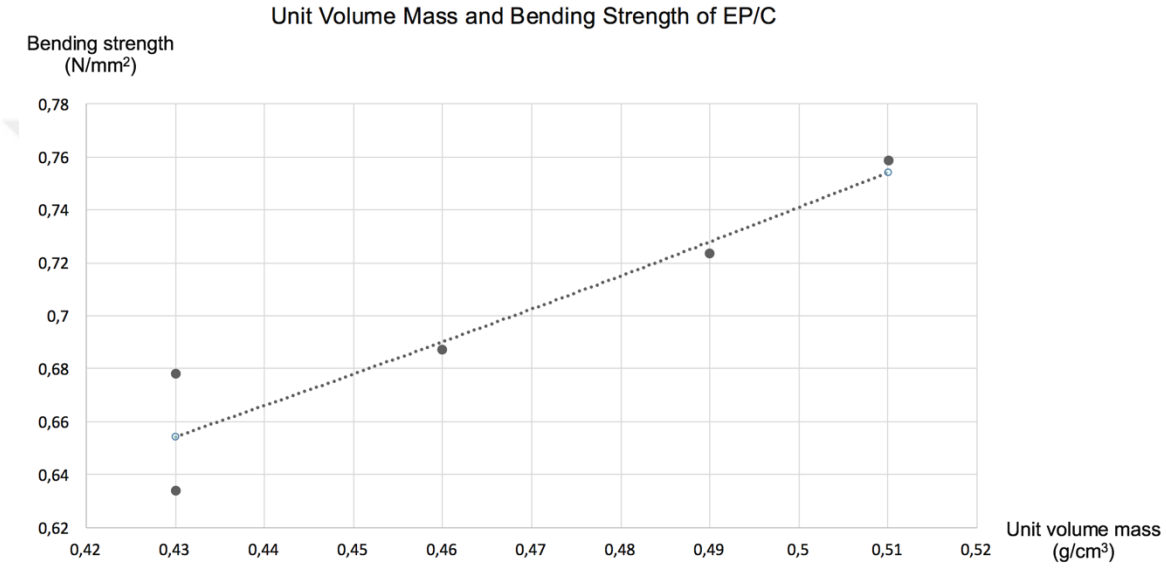

Figure 27 The specific gravity and bending strength of EP/C control sample boards

Similarly, some of the AEP/C boards with the same UVM values had a bending strength of 0.62, 0.66, and 0.74 N/mm^2 as shown in Figure 28. A bit UVM increases, 0.56 g/cm^3 leaded slight increase on the bending strength as 0.77 N/mm^2. The upward trend was also valid for the board with a density of 0.58 g/cm^3 and a corresponding bending strength value of 0.84 N/mm^2. The different

flexural strength of the boards with the same UVM value can be explained by the similar reasons aforementioned for the EP/C board graph.

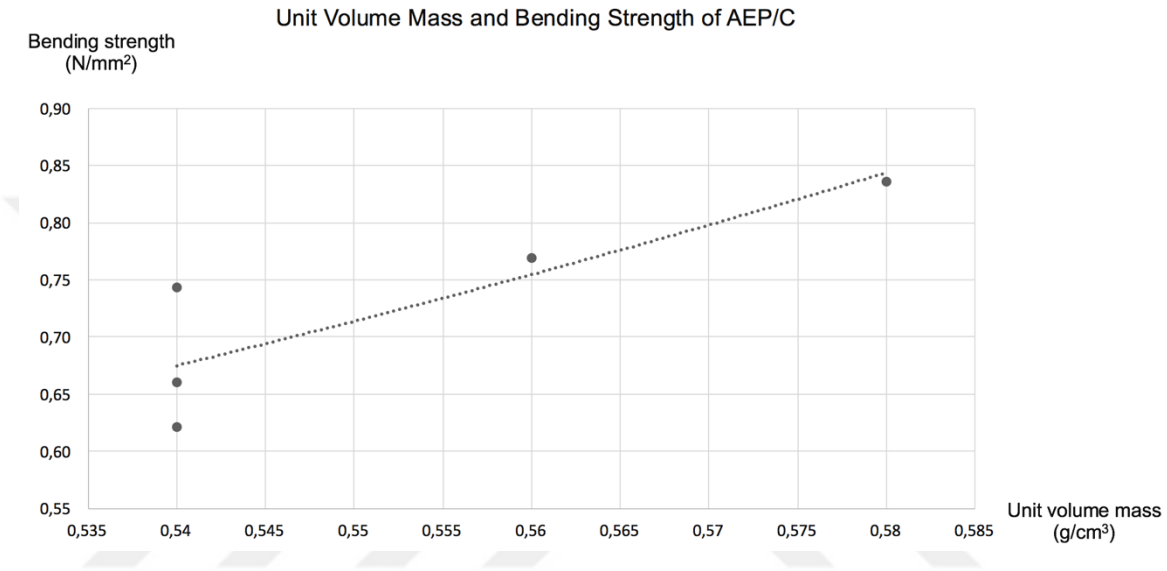

Figure 28 The specific gravity and bending strength of AEP/C control sample boards

The mean of UVM of EP/C control board sample was 0.46 ± 0.02 g/cm^3, and AEP/C boards was 0.55 ± 0.01 g/cm^3. The mean values of bending strengths for EP/C and AEP/C were 0.7 ± 0.02 N/mm^2 and 0.73 ± 0.04 N/mm^2, respectively. The increase of ~0.09 g/cm^3 on UVM mean values caused ~0.03 N/mm^2 increase on the flexural strengths. These contributions were only considered even insignificant. In other words, while the board densities slightly increased by the aerogel modification, their mechanical strengths were almost the same.

The mechanical strength of the EP/C boards were examined in the previous study (Yilmazer, 2019). In common in this and our study, the flexural strength increased as the density increased. The flexural strength of the EP/C board was 0.52 N/mm^2 in this study. Our study proposes EP/C board with 0.7 ± 0.02 N/mm^2 bending strength that was higher than the previous study. The difference can be rooted from the type and thus the physical properties of EPA used in studies. The second reason can be the cooling duration difference in the annealing processes. In fact, the annealing process applied to the boards in this study is the same as in the previous study as 5 hours heating up to 550 °C, 5 hours heating from 550 to 850 °C, 4 hours of constant heating on 850 °C. When the process is completed, it is significant for the boards to cool down from 850 °C to room temperature without any intervention. However, this long cooling period causes the boards to be cured by being exposed to these temperatures for a long time. It can be concluded that the boards in this study had higher density at the end of the process (compared to the previous study) because of the additional curing by staying in the cooling phase for a longer time. The increase in mechanical strength with the increase in density in the boards was observed in the graphs of in the study of Yilmazer (2018). The ratios of EPA, clay and DH_2O required for the preparation of the boards, whole physical and mechanical characterization results of the EP/C and AEP/C boards are demonstrated in Table 6.

The hypothesis of this research offered a contribution to the mechanical strength of clay-based aerogel-modified expanded perlite board. However, the aerogel modification could not have a significant effect on both UVM and the bending strength of boards. This means that the performance of aerogel-modified boards cannot be affected by density-dependent variables. Moreover, the thermal conductivity of aerogel is lower than air. Therefore, the thermal insulation performance of boards is promising and should be measured in future study. The limit bending strength value of external board products is 9 N/mm^2. Future research may offer solutions to reach this value. This limit can be achieved by designing the boards with physical alternatives such as sandwich composite. Another solution would be reinforcement on AEP/C boards with geothermal materials such as fly ash, or using materials with high mechanical strength such as cement as a matrix.

Table 6 Material ratios for board preparation and physical and mechanical test results of EP/C and AEP/C boards

Physical and mechanical test results											
Property	Perlite	Clay	Perlite	Clay	DH_2O	Unit volume mass (UVM)	Specific gravity (SP)	Volume of voids (V_V)	Porosity (n)	Water absorption (WA)	Bending strength (σ)
Unit / Sample	% (W/W)	% (W/W)	g	g	g	g/cm^3	g/cm^3	cm^3	%	%	N/mm^2
EP/C (Control sample)	50	50	80	80	135	0.46 ± 0.01	2.33 ± 0.02	40.51	0.78	86.28	0.7 ± 0.02
AEP/C	50	50	80	80	125	0.55 ± 0.01	2.36 ± 0.01	36.23 ± 1.05	0.77	83.91 ± 0.49	0.73 ± 0.04

CHAPTER V

CONCLUSION

This thesis aims to produce an aerogel-modified expanded perlite and clay board (AEP/C) and investigate the physical and mechanical properties of the board. The concentration of acid catalyst and the amount of base catalyst in the sol-gel synthesis were systematically investigated. The optimum amounts, durations, ratios for other variables in sol-gel steps were examined in light of previous studies. The aerogel synthesis recipe was used for the AEP production. After ensuring the characterization and tests of AEP, these particles were mixed with the clay matrix to form AEP/C composite board. The characterization and test results demonstrated that the production of the AEP/C board was successfully acquired. Some significant findings of this research are summarized as follows.

1. The optimization of aerogel synthesis was carried to prepare the starting recipe for AEP. The concentration of acid catalyst and amount of base catalysts were studied. The optimum concentration of acid catalyst was

determined as 0.02 M with the base catalyst molarity of 1 M. The amount of acid catalyst was 10 ml, and of base catalyst was 5 ml.

2. The amount of EPA requires to constitute aerogel both filling and covering the surface of a specific amount of solvent mixture was studied for AEP synthesis. The amounts of solvents and agents were 2 ml TEOS, 125 ml EtOH, 10 ml acid catalyst, 5 ml base catalyst. The required amount of EPA for the synthesis were determined as 40 g.

3. The sintering test of AEP particles was carried by the AEP/C board annealing process which is 5 hours heating up to 550 °C, 5 hours heating from 550 to 850 °C, 4 hours of constant heating on 850 °C. Additionally, 1100 °C heat treatment was applied to the particles. The results demonstrated that the aerogel coverage on the surface of perlite prevented the shrinkage and the sintering of particles. Therefore, AEP particles retained white color and volume of their structure after heat treatment while EPA particles turned to pinkish color and shrank. This is promising that AEP can withstand high-temperature fire situations. Scanning electron microscope was used to characterize the surface morphologies of both EPA, EPA after high-temperature annealing, and AEP. The sintering of EPA leaded the flattened surface structures on the particles.

4. The loose bulk density of AEP particles was determined in accordance with TS EN 1097-3 standard, and the specific gravities were measured by

Le Chatelier flask in accordance with TS 2511 standard. The loose bulk density of EPA samples was 0.21 g/cm^3 and AEP was calculated as 0.26 ± 0.01 g/cm^3. The specific gravity of EPA samples was 1.8 ± 0.01 g/cm^3 and AEP was 1.93 ± 0.09 g/cm^3. The aerogel modification of EPA slightly increased both loose bulk density and specific gravity of the particles.

5. The interior surface morphologies of EP/C and AEP/C boards were diagnosed by scanning electron microscope. The aerogel modification was clearly seen inside perlite pores and the clay coverage on the surface was observed.

6. The unit volume mass calculations were carried for of EP/C control board and AEP/C board samples. The unit volume mass of EP/C was 0.46 ± 0.02 g/cm^3 while this value was 0.55 ± 0.01 g/cm^3 for AEP/C boards. The aerogel modification caused a slight increase in the unit volume mass.

7. The specific gravity of AEP/C boards was measured by using the Le Chatelier flask in accordance with TS 2511 standard. According to the calculations, the mean specific gravity of EP/C sample (control sample) was 2.33 ± 0.02 and AEP/C was 2.36 ± 0.01. The specific gravity of the boards was almost equal.

8. The water absorption tests of boards were carried according to TS EN ISO 29767 standard. According to calculations, the volume of voids of the EP/C board is 40.51, and 36.23 ± 1.05 for the AEP/C composite board. The void volume was decreased by aerogel modification. On the other

hand, the porosities of the boards were almost equal; 0.78% for EP/C and 0.77%for AEP/C. The water absorption of the EP/C was 86.28% and the AEP/C board was 83.91 ± 0.49%. The contribution of aerogel modification to these values can be neglected.

9. The bending strength of boards was determined by a 3-point flexural test. The bending-stress measuring equipment was used to acquire the test. The flexural strength of AEP/C boards was 0.73 ± 0.04 N/mm^2 and the bending strength of the EP/C board was 0.7 ± 0.02 N/mm^2. The aerogel modification slightly affected the bending strength of the boards.

10. There were slight UVM changes of the boards prepared with AEP and clay. These rather insignificant density changes also did not result in significant flexural strength increases. Therefore, while the density-related properties can be maintained, the thermal insulation performances of AEP/C boards should be determined. While the thermal insulation advantages of aerogel modification are controlled, the reinforcement should be provided on boards. New material added to the board mixture, changing the matrix with high mechanical strength, or designing a new sandwich composite would be solutions.

REFERENCES

Abu-Jdayil, B., Mourad, A. H., Hittini, W., Hassan, M., & Hameedi, S. (2019). Traditional, state-of-the-art and renewable thermal building insulation materials: An overview. *Construction and Building Materials, 214*, 709–735. https://doi.org/10.1016/j.conbuildmat.2019.04.102

Aditya, L., Mahlia, T. M. I., Rismanchi, B., Ng, H. M., Hasan, M. H., Metselaar, H. S. C., Muraza, O., & Aditiya, H. B. (2017). A review on insulation materials for energy conservation in buildings. *Renewable and Sustainable Energy Reviews, 73,* 352–1365. https://doi.org/10.1016/j.rser.2017.02.034

Afshari, H., Ashraf, S., Ebadi, A. G., Jalali, S., Abbaspour, H., Daliri, M. S., & Rasool Toudar, S. (2011). Study of the effects irrigation water salinity and pH on production and relative absorption of some elements nutrient by the tomato plant. *American Journal of Applied Sciences*, *8*(8), 766–772.

Ahmed, M. (2015). *Development of structural lightweight concrete utilizing local materials* (Master's thesis). https://eprints.kfupm.edu.sa/id/eprint/139529/

Alkan, M., & Doğan, M. (2001). Adsorption of copper(II) onto perlite. *Journal of Colloid and Interface Science*, *243*(2), 280–291. https://doi.org/10.1006/jcis.2001.7796

Al-Homoud, M. S. (2005). Performance characteristics and practical applications of common building thermal insulation materials. *Building and Environment*, *40*(3), 353–366. https://doi.org/10.1016/j.buildenv.2004.05.013

Austin, G. S., & Barker, J. M. (1998). *New Mexico Geological Society Commercial perlite deposits of New Mexico and North America Annual NMGS Fall Field Conference Guidebooks*.

http://nmgs.nmt.edu/publications/guidebooks/49

Begum, H., Horoshenkov, K. V., Conte, M., Malfait, W. J., Zhao, S., Koebel, M. M., Bonfiglio, P., & Venegas, R. (2021). The acoustical properties of tetraethyl orthosilicate based granular silica aerogels. *The Journal of the Acoustical Society of America*, *149*(6), 4149–4158. https://doi.org/10.1121/10.0005200

Binici, H., & Kalaycı, F. (2015). Production of perlite based thermal insulation material. *International Journal of Academic Research and Reflection, 3(7)*, 47–54.

Bribián, I. Z. , Capilla, A. V., & Usón, A. A. (2011). Life cycle assessment of building materials: Comparative analysis of energy and environmental impacts and evaluation of the eco-efficiency improvement potential. *Building and Environment*, *46*(5), 1133–1140. https://doi.org/10.1016/j.buildenv.2010.12.002

Brinker, C. J., & Scherer, G. W. (1990). *Sol-gel science, the physics and chemistry of sol-gel processing*. San Diego, CA: Academic Press.

Buisson, P., Hernandez, C., Pierre, M., & Pierre, A. C. (2001). Encapsulation of lipases in aerogels. *Journal of Non-Crystalline Solids, 285*(1), 295–302. http://dx.doi.org/10.1016/S0022-3093(01)00470-7

Burger, T., & Fricke, J. (1998). Aerogels: Production, modification and applications. *Berichte der Bunsengesellschaft/Physical Chemistry Chemical Physics, 102(11)*, 1523–1528. http://dx.doi.org/10.1002/bbpc.19981021102

Celik, A. G., Kilic, A. M., & Cakal, G. O. (2013). Expanded perlite aggregate characterization for use as a lightweight construction raw material. *Physicochemical Problems of Mineral Processing, 49*(2), 689–700. https://doi.org/10.5277/ppmp130227

Chan, K. K., & Brownsten, A. M. (1991). Ceramic membranes-growth prospects and opportunities. *American Ceramic Society Bulletin, 70*, 703–707.

Chen, F., Zhang, Y., Liu, J., Wang, X., Chu, P. K., Chu, B., & Zhang, N. (2020). Fly ash based lightweight wall materials incorporating expanded perlite/SiO_2 aerogel composite: Towards low thermal conductivity. *Construction and Building Materials*, *249*. https://doi.org/10.1016/j.conbuildmat.2020.118728

Ciampi, M., Leccese, F., & Tuoni, G. (2003). Ventilated facades energy performance in summer cooling of buildings. *Solar Energy*, *75*(6), 491–502. https://doi.org/10.1016/j.solener.2003.09.010

Ciullo, P. A. (1996). Industrial minerals and their uses: a handbook and formulary. Westwood, N.J. : Noyes Publications.

Coma, J., Pérez, G., Solé, C., Castell, A., & Cabeza, L. F. (2016). Thermal assessment of extensive green roofs as passive tool for energy savings in buildings. *Renewable Energy, 85*, 1106–1115. https://doi.org/10.1016/j.renene.2015.07.074

Cox, P. M., Betts, R. A., Jones, C. D., Spall, S. A., & Totterdell, I. J. (2000). Erratum: Acceleration of global warming due to carbon-cycle feedbacks in a coupled climate model. *Nature 408*(750), 184–187. https://doi.org/10.1038/35047138

Cuce, E., Cuce, P. M., Wood, C. J., & Riffat, S. B. (2014a). Optimizing insulation thickness and analysing environmental impacts of aerogel-based thermal superinsulation in buildings. *Energy and Buildings*, *77*, 28–39. https://doi.org/10.1016/j.enbuild.2014.03.034

Cuce, E., Cuce, P. M., Wood, C. J., & Riffat, S. B. (2014b). Toward aerogel based thermal superinsulation in buildings: A comprehensive review. In *Renewable and Sustainable Energy Reviews, 34*, 273–299. https://doi.org/10.1016/j.rser.2014.03.017

Dawood, E. T. (2015). Experimental study of lightweight concrete used for the production of canoe. *Al-Rafidain Engineering Journal, 23(2)*, 96–106. http://dx.doi.org/10.33899/rengj.2015.101085

Doğan M., & Alkan M. (2004). Some physicochemical properties of perlite as an adsorbent. *Fresenius Environmental Bulletin, 13,* 252–257.

Dongmei, P., Mingyin, C. Himing, D., & Zhongping, L. (2012). The effects of external wall insulation thickness on annual cooling and heating energy uses under different climates. *Applied Energy, 97*, 313–318.

Dorcheh, S. A., & Abbasi, M. H. (2008). Silica aerogel; synthesis, properties and characterization. *Journal of Materials Processing Technology, 199*(1), 10–26. https://doi.org/10.1016/j.jmatprotec.2007.10.060

Doroudiani, S., & Kortschot, M. T. (2003). Polystyrene foams. I. Processing-structure relationships. *Journal of Applied Polymer Science, 90*, 1412–1420. https://doi.org/10.1002/app.12804

Doroudiani, S., & Omidian, H. (2010). Environmental, health and safety concerns of decorative mouldings made of expanded polystyrene in buildings. *Building and Environment, 45*(3), 647–654.

Ennis, D. J. (2011). Perlite mining and reclamation in the no aqua peaks, Taos County, New Mexico. *New Mexico Geological Society Guidebook, 62nd Field Conference Geology of Tusas Mountains-Ojo Caliente*. 409–418.

Fricke, J., & Tillotson, T. (1997). Aerogels: production, characterization, and applications. *Thin Solid Films, 297*(1–2), 212–223. https://doi.org/10.1016/S0040-6090(96)09441-2

Haery, H. A. (2017). *Elastic and mechanical properties of expanded perlite and perlite/epoxy foams* (Doctoral dissertation). https://ogma.newcastle.edu.au/vital/access/manager/Repository/uon:28964

Hilonga, A., Kim, J. K., Sarawade, P. B., & Kim, H. T. (2009). Low-density TEOS-based silica aerogels prepared at ambient pressure using isopropanol as the preparative solvent. *Journal of Alloys and Compounds, 487*(1-2), 744–750.

Hüsing, N., & Schubert, U. (1998). Aerogels-airy materials: chemistry, structure, and properties. *Angewandte Chemie International Edition, 37(1-2)*, 22–45.

10.1002/(SICI)1521-3773(19980202)37:1/2<22::AID-ANIE22>3.0.CO;2-I

Ingrao, C., Messineo, A., Beltramo, R., Yigitcanlar, T., & Ioppolo, G. (2018). How can life cycle thinking support sustainability of buildings? Investigating life cycle assessment applications for energy efficiency and environmental performance. *Journal of Cleaner Production, 201*, 556–569. https://doi.org/10.1016/j.jclepro.2018.08.080

Ioppolo, G., Cucurachi, S., Salomone, R., Saija, G., & Shi, L. (2016). Sustainable local development and environmental governance: a strategic planning experience. *Sustainability, 8*(2), 180. https://doi.org/10.3390/su8020180

Ishizaki, K., Komarneni, S., & Nanko, M. (2013). *Porous materials: Process technology and applications*. Tokyo: Springer Science & Business Media.

Işıkdağ, B., Topçu, B., & Gökbel, S. (2015). Characterization of mortars produced with expanded perlite, slaked lime and waste tile dust. *Iwcea Özel Sayisi (1)*, 29–42.

Jedidi, M., Benjeddon, O., & Soussi, C. (2015). Effect of expanded perlite aggregate dosage on properties of lightweight concrete. *Jordon Journal of Civil Engineering, 9(3)*, 278–291.

Jia, G., & Li, Z. (2021). Influence of the aerogel/expanded perlite composite as thermal insulation aggregate on the cement-based materials: Preparation, property, and microstructure. *Construction and Building Materials*, *273,* 121728. https://doi.org/10.1016/j.conbuildmat.2020.121728

Jia, G., Li, Z., Liu, P., & Jing, Q. (2018). Preparation and characterization of aerogel/expanded perlite composite as building thermal insulation material. *Journal of Non-Crystalline Solids*, *482,* 192–202. https://doi.org/10.1016/j.jnoncrysol.2017.12.047

Johnstone, S. J., & Johnstone, M.G. (1961). *Minerals for the chemical and allied industries* (2nd ed.). London, UK: Chapman and Hall.

Kalhor, K., & Emaminejad, N. (2020). Qualitative and quantitative optimization of

thermal insulation materials: Insights from the market and energy codes. *Journal of Building Engineering, 30*, 101275. https://doi.org/10.1016/j.jobe.2020.101275

Kanamori, K. (2011). *Organic-inorganic hybrid aerogels with high mechanical properties via organotrialkoxysilane-derived sol-gel process*. *Journal of the Ceramic Society of Japan, 119*(1385),16–22. https://doi.org/10.2109/jcersj2.119.16

Kim, S. M., Chakrabarti, K., Oh, E. O., & Whang, C. M. (2003). Effects of pH during the base catalyzed reaction of two-step acid/base catalyzed process on the microstructures and physical properties of poly(dimethylsiloxane) modified silica xerogels. *Journal of Sol-Gel Science and Technology, 27*, 149–155. https://doi.org/10.1023/A:1023794300032.

Kim, S., Seo, J., Cha, J., & Kim, S. (2013). Chemical retreating for gel-typed aerogel and insulation performance of cement containing aerogel. *Construction and Building Materials*, *40*, 501–505. https://doi.org/10.1016/j.conbuildmat.2012.11.046

Koebel, M., Rigacci, A., & Achard, P. (2012). Aerogel-based thermal superinsulation: An overview. *Journal of Sol-Gel Science and Technology, 63*(3), 315–339. https://doi.org/10.1007/s10971-012-2792-9

Kusiorowski, R., Witek, J., Majchrowicz, I., Kleta, A., & Jirsa-Ociepa, A. (2019). Fire barrier based on expanded perlite composites. *13th International Conference Modern Building Materials, Structures and Techniques*. May 16-17, 2019. Vilnius, Lithuania. https://doi.org/10.3846/mbmst.2019.047

Lanzón, M., & García-Ruiz, P.A. (2008). Lightweight cement mortars: Advantages and inconveniences of expanded perlite and its influence on fresh and hardened state and durability. *Construction and Building Materials, 22*(8)*,* 1798–1806. https://doi.org/10.1016/j.conbuildmat.2007.05.006

Ma, H. S., Roberts, A. P., Evost, C., Emi Jullien, J. H., & Scherer, G. W. (2000).

Mechanical structure-property relationship of aerogels. *Journal of Non-Crystalline Solids, 277*(2-3), 127–141. https://doi.org/10.1016/S0022-3093(00)00288-X

Maaloufa, Y., Mounir, S., Khabbazi, A., Kettar, J., & Khaldoun, A. (2015). Thermal characterization of materials based on clay and granular: cork or expanded perlite. *Energy Procedia*, *74*, 1150–1161. https://doi.org/10.1016/j.egypro.2015.07.757

Mazraeh-shahi, Z. T., Shoushtari, A. M., & Bahramian, A. R. (2015). A new approach for synthesizing the hybrid silica aerogels. *Procedia Materials Science*, *11*, 571–575. https://doi.org/10.1016/j.mspro.2015.11.072

Ortiz, O., Castells, F., & Sonnemann, G. (2009). Sustainability in the construction industry: a review of recent developments based on LCA. *Construction and Building Materials, 23*(1), 28–39. https://doi.org/10.1016/j.conbuildmat.2007.11.012

Otis, L. M. (1960). *Perlite, in Mineral facts and problems*. Washington, WA: United states Government Printing Office.

Öztürk, Z. B. (2017). Effect of addition of Avanos's (Nevşehir) clays on physical and microstructure of ceramic tile. *Journal of Australian Ceramic Society, 53*, 101–107.

Papadopoulos, A. M. (2005). State of the art in thermal insulation materials and aims for future developments. *Energy and Buildings*, *37*(1), 77–86. https://doi.org/10.1016/j.enbuild.2004.05.006

Parmenter, K. E., & Milstein, F. (1998). Mechanical properties of silica aerogels. *Journal of Non-Crystalline Solids, 223*(3), 179–189. https://doi.org/10.1016/S0022-3093(97)00430-4

Peng, K., & Yang, H. (2013). Preparation of aerogel-modified expanded perlite and its application in heat insulation coating. *Advanced Materials Research*, *668*, 360–364. http://dx.doi.org/10.4028/www.scientific.net/AMR.668.360

Pierre, A.C., & Rigacci, A. (2011). SiO2 Aerogels. In: Aegerter M., Leventis N., Koebel M. (eds) Aerogels Handbook. *Advances in Sol-Gel Derived Materials and Technologies* (pp. 21–45). Springer, New York, NY. https://doi.org/10.1007/978-1-4419-7589-8_2

Rao, V. A., & Bhagat, S. D. (2004). Synthesis and physical properties of TEOS-based silica aerogels prepared by two-step (acid-base) sol-gel process. *Solid State Sciences, 6*(9), 945–952. https://doi.org/10.1016/j.solidstatesciences.2004.04.010

Rashad, A. M. (2016). A synopsis about perlite as building material - A best practice guide for Civil Engineer. *Construction and Building Materials, 121,* 338–353. https://doi.org/10.1016/j.conbuildmat.2016.06.001

Rashad, A. M. (2018). Lightweight expanded clay aggregate as a building material – An overview. *Construction and Building Materials 170*, 757–775. https://doi.org/10.1016/j.conbuildmat.2018.03.009

Riffat, S. B., & Qiu, G. (2013). A review of state-of-the-art aerogel applications in buildings. *International Journal of Low-Carbon Technologies*, *8*(1), 1–6. https://doi.org/10.1093/ijlct/cts001

Roulia, M., Chassapis, K., Fotinopoulos, C., Savvidis, T., & Katakis, D. (2003). Dispersion and sorption of oil spills by emulsifier-modified expanded perlite. *Spill Science and Technology Bulletin*, *8*(5–6), 425–431. https://doi.org/10.1016/S1353-2561(02)00066-X

Sarawade, P. B., Kim, J., Kim, H., & Kim, H. (2007). High specific surface area TEOS-based aerogels with large pore volume prepared at an ambient pressure. *Applied Surface Science, 254,* 574–579.

Sengul, O., Azizi, S., Karaosmanoglu, F., & Tasdemir, M. A. (2011). Effect of expanded perlite on the mechanical properties and thermal conductivity of lightweight concrete. *Energy and Buildings*, *43*(2–3), 671–676. https://doi.org/10.1016/j.enbuild.2010.11.008

Shi, F., Wang, L., & Liu, J. (2006). Synthesis and characterization of silica aerogels by a novel fast ambient pressure drying process. *Materials Letters, 60*(29-30), 3718–3722. http://dx.doi.org/10.1016/j.matlet.2006.03.095

Singh, M., & Garg, M. (1991). Perlite-based building materials-a review of current applications. C*onstruction and Building Materials, 5*(2). 75–81. https://doi.org/10.1016/0950-0618(91)90004-5

Stazi, F., Tomassoni, F., Vegliò, A., & Di Perna, C. (2011). Experimental evaluation of ventilated walls with an external clay cladding. *Renewable Energy, 36*(12), 3373–3385.

Stec, A. A., & Hull, T.R. (2011). Assessment of the fire toxicity of building insulation materials. *Energy and Buildings 43*, 498–506. https://doi.org/10.1016/j.enbuild.2010.10.015

Stefanidou, M., & Pachta, V. (2020). Influence of perlite and aerogel addition on the performance of cement-based mortars at elevated temperatures. *IOP Conference Series: Earth and Environmental Science*, *410*(1). https://doi.org/10.1088/1755-1315/410/1/012111

Stergar, J., & Maver, U. (2016). Review of aerogel-based materials in biomedical applications. *Journal of Sol-Gel Science Technology, 77*, 738–752. https://doi.org/10.1007/s10971-016-3968-5

Sulong, R. Mustapa, N. H., & Abdul Rashid, M. K. (2019). Application of expanded polystyrene (EPS) in buildings and constructions: A review. *Journal of Applied Polymer Science, 136*, 47529.

Taherishargh, M., Belova, I. V., Murch, G. E., & Fiedler, T. (2014). Low-density expanded perlite-aluminium syntactic foam. *Materials Science and Engineering A*, *604*, 127–134. https://doi.org/10.1016/j.msea.2014.03.003

Topçu, I. B., & Işikdağ, B. (2007). Manufacture of high heat conductivity resistant clay bricks containing perlite. *Building and Environment*, *42*(10), 3540–3546. https://doi.org/10.1016/j.buildenv.2006.10.016

Topçu, I. B., & Işikdağ, B. (2008). Effect of expanded perlite aggregate on the properties of lightweight concrete. *Journal of Materials Processing Technology*, *204*(1–3), 34–38. https://doi.org/10.1016/j.jmatprotec.2007.10.052

TS EN ISO 29767. Thermal insulating products for building applications - Determination of short-term water absorption by partial immersion.

TS EN 1097-3. Tests for mechanical and physical properties of aggregates- Part 3: Determination of loose bulk density and voids.

TS EN 12089. Thermal insulating products for building applications- Determination of bending behavior.

TS EN 13169+1. Thermal insulation products for buildings - Factory made expanded perlite board (EPB) products - Specification.

TS 2511. Mix design for structural lightweight aggregate concrete.

Tsilingiris, P. T. (2006). Wall heat loss from intermittently conditioned spaces-The dynamic influence of structural and operational parameters. *Energy and Buildings*, *38*(8), 1022–1031. https://doi.org/10.1016/j.enbuild.2005.11.012

Türkmen, I., & Kantarcı, A. (2007). Effects of expanded perlite aggregate and different curing conditions on the physical and mechanical properties of self-compacting concrete. *Building and Environment 42(6)*, 2378–2383. https://doi.org/10.1016/j.buildenv.2006.06.002

Veres, P., López-Periago, A. M., Lázár, I., Saurina, J., & Domingo, C. (2015). Hybrid aerogel preparations as drug delivery matrices for low water-solubility drugs. *International Journal of Pharmaceutics*, *496*(2), 360–370. https://doi.org/10.1016/j.ijpharm.2015.10.045

Wang, X., & Jana, S. C. (2013). Synergistic hybrid organic–inorganic aerogels. *ACS Appl Mater Interfaces 5*(13), 6423–6429. https://doi.org/10.1021/am401717s.

Wang, L., Li, Z., Jing, Q., & Liu, P. (2018). Synthesis of composite insulation materials—expanded perlite filled with silica aerogel. *Journal of Porous Materials*, *25*(2), 373–382. https://doi.org/10.1007/s10934-017-0448-4

Wang, L., Liu, P., Jing, Q., Liu, Y., Wang, W., Zhang, Y., & Li, Z. (2018). Strength properties and thermal conductivity of concrete with the addition of expanded perlite filled with aerogel. *Construction and Building Materials*, *188*, 747–757. https://doi.org/10.1016/j.conbuildmat.2018.08.054

Wu, G., Yu, Y., Cheng, X., & Zhang, Y. (2011). Preparation and surface modification mechanism of silica aerogels via ambient pressure drying. *Materials Chemistry and Physics, 129*(1), 308–314. https://doi.org/10.1016/j.matchemphys.2011.04.003

Xu, X., Zhang, Y., Lin, K., Di, H., & Yang, R. (2005). Modeling and simulation on the thermal performance of shape-stabilized phase change material floor used in passive solar buildings. *Energy and Buildings, 37*(10), 1084–1091.

Yıldızel, S.A. (2018). Mechanical performance of glass fiber reinforced composites made with gypsum, expanded perlite and silica sand. *Romanian Journal of Materials, 48*, 229–235.

Yılmazer, S. (1998). *Perlitli akustik plakaların nemli ortamlardaki davranışları.* Doctoral dissertation). Karadeniz Technical University.

Yılmazer, S. (2018). *The optimization of thermal insulation board made of clay based expanded perlite (EPcB)*. TUBITAK 1001 Project Final Report.

Yilmazer, S. (2019). The chemical synthesis and process optimization of a porous thermal insulation board made of clay based expanded perlite (EPcB). *International Porous Powder Materials Symposium and Exhibition (PPM), October, 9-11*. Marmaris, Muğla, Turkey.

Yılmazer, S., & Baytekin, B. (2017). The mixture ratio optimization of expanded perlite-clay based board (EPcB) for thermal resistance performance. *International Porous Powder Materials Symposium and Exhibition (PPM),*

İzmir Institute of Technology, September,12-15. Kuşadası, İzmir, Turkey.

Zou, C., Zhang, G., Zhu, R., Yuan, X., Zhao, X., Hou, L., Wen, B., & Wu, X. (2013). Characteristics of Volcanic Reservoirs. *Volcanic Reservoirs in Petroleum Exploration,* (pp. 31–90). Elsevier. https://doi.org/10.1016/b978-0-12-397163-0.00003-8